TECHNICAL REPORT STANDARD TITLE PAGE

1. Report No.	2. Government Accession No.	3. Recipient's Catalog No.
TTI-2-5-76-31-1F		

4. Title and Subtitle	5. Report Date
TRANSDUCERS FOR MEASUREMENT OF PILE FORCES	March, 1977
	6. Performing Organization Code

7. Author(s)	8. Performing Organization Report No.
Richard E. Bartoskewitz, Lionel J. Milberger, and Harry M. Coyle	Research Report 31-1F

9. Performing Organization Name and Address	10. Work Unit No.
Texas Transportation Institute Texas A&M University College Station, Texas 77843	11. Contract or Grant No. Research Study 2-5-76-31
	13. Type of Report and Period Covered
12. Sponsoring Agency Name and Address Texas State Department of Highways and Public Transportation Transportation Planning Division P. O. Box 5051; Austin, Texas 78763	Final - September, 1975 March, 1977
	14. Sponsoring Agency Code

15. Supplementary Notes

Research performed in cooperation with DOT, FHWA.
Research Study Title: Development of a Transducer for Use in Measuring Peak Forces on Piles During Driving.

16. Abstract

An aluminum load cell was designed and constructed for the purpose of measuring the peak force that is developed at the top of a pile during driving. The load cell can be used on square concrete piles up to 16-in. (410-mm) square. It contains 9 sensing elements distributed over the active area to accurately measure inclined or eccentric loadings. The load cell is relatively lightweight and portable, and was designed to interface with an electronic peak force readout unit that was designed and constructed on an earlier project.

An alternate peak force transducing means was model tested in the laboratory and field tested on full-scale piles. The method utilizes encapsulated electric resistance strain gages rigidly bonded to the exterior pile surface with a rapid-setting epoxy. Test data consisting of driving records and maximum pile forces at the pile heads are presented for four 55-ft (17-m) long piles driven in soft silty clay. An example wave equation problem is presented to illustrate the application and use of the measured peak force.

17. Key Words	18. Distribution Statement
Bearing Capacity, Force Transducer, Load Cell, Peak Dynamic Pile Force, Pile Driving, Wave Equation Analysis	No Restrictions. This document is available to the public through the National Technical Information Service, Springfield, Virginia 22161.

19. Security Classif. (of this report)	20. Security Classif. (of this page)	21. No. of Pages	22. Price
Unclassified	Unclassified	68	

Form DOT F 1700.7 (8-69)

TRANSDUCERS FOR MEASUREMENT OF PILE FORCES

by

Richard E. Bartoskewitz
Engineering Research Associate

Lionel J. Milberger
Research Associate

and

Harry M. Coyle
Research Engineer

Research Report No. 31-1F

Development of a Transducer for Use In
Measuring Peak Forces On Piles During Driving
Research Study Number 2-5-76-31

Sponsored by the
State Department of Highways and Public Transportation
in Cooperation with the
U. S. Department of Transportation
Federal Highway Administration

March 1977

TEXAS TRANSPORTATION INSTITUTE
Texas A&M University
College Station, Texas

DISCLAIMER

The contents of this report reflect the views of the authors who are responsible for the facts and the accuracy of the data presented herein. The contents do not necessarily reflect the official views or policies of the Federal Highway Administration. This report does not constitute a standard, specification, or regulation.

ABSTRACT

An aluminum load cell was designed and constructed for the purpose of measuring the peak force that is developed at the top of a pile during driving. The load cell can be used on square concrete piles up to 16-in. (410-mm) square. It contains 9 sensing elements distributed over the active area to accurately measure inclined or eccentric loadings. The load cell is relatively lightweight and portable, and was designed to interface with an electronic peak force readout unit that was designed and constructed on an earlier project.

An alternate peak force transducing means was model tested in the laboratory and field tested on full-scale piles. The method utilizes encapsulated electric resistance strain gages rigidly bonded to the exterior pile surface with a rapid-setting epoxy. Test data consisting of driving records and maximum pile forces at the pile heads are presented for four 55-ft (17-m) long piles driven in soft silty clay. An example wave equation problem is presented to illustrate the application and use of the measured peak force.

KEY WORDS: Bearing Capacity, Force Transducer, Load Cell, Peak Dynamic Pile Force, Pile Driving, Wave Equation Analysis

SUMMARY

The information presented in this report was obtained during a one-year type B study. This study was conducted to develop a transducer that can be used with the DHT dynamic peak pile force readout which was constructed during an earlier study in 1973-74. The transducer and the readout unit are used to measure the peak force that is developed at the head of a pile during driving. The measured peak force is then used in a wave equation analysis of the hammer-pile-soil system to adjust the pile and cushion stiffnesses so that the computed peak force matches the measured peak force. A bearing graph can then be developed for predicting pile bearing capacity.

An aluminum load cell was designed and constructed for use on square concrete piles up to 16-in. (410-mm) square. The load cell is relatively lightweight, weighing about 88-lb (40-kg), and can be easily transported and handled without need of heavy equipment. The load cell contains no moving parts, thereby reducing maintenance and upkeep costs. The design of the load cell is discussed and design drawings are included.

An alternate transducing method was tested for use on concrete piles. The method uses embedment type strain gages rigidly attached to the side of the pile. Laboratory tests were conducted to determine the correlation between internal and external gages. Field tests were conducted near High Island, Texas, using rapid-setting epoxy to bond the gages to the pile surface. Complete field test data are included, and an example wave equation problem is presented to illustrate the use of measured peak forces.

IMPLEMENTATION STATEMENT

The load cell that was designed and constructed for use with the DHT dynamic peak force readout unit is available to DHT for immediate implementation and use. The load cell connects directly to the readout unit by means of a multipin connector. The entire system can be assembled and ready for use in a short period of time. The calibration and operation procedures for the readout unit can be learned in a matter of minutes by any competent person even though that person may lack any previous experience with electronic instruments.

The use of strain gages that are rigidly bonded to the exterior surface of a pile has been shown to be a reliable method for measuring the peak pile force, and the use of this method is recommended whenever field conditions preclude the use of the load cell. This method is more time consuming due to the fact that some time must be allowed for the bonding agent to fully harden, however this time can be minimized by proper planning procedures.

It is recommended that either one or both of these procedures be implemented as soon as possible to provide opportunities for field personnel to become acquainted with the equipment and techniques, and to provide a broad base of experience for design personnel in utilizing the information. The use of these devices will add a new dimension in flexibility to the use of the wave equation method of piling analysis, a method which is now being used by DHT and numerous other institutions and agencies, both public and private, for design and analysis of pile-supported structures.

TABLE OF CONTENTS

LIST OF FIGURES

INTRODUCTION

Background and Prior Research - - In the early 1960's the Texas Highway Department was experiencing problems with concrete piles cracking during the process of driving. In many cases the piles were cracked or damaged to the extent that they were no longer serviceable. A cooperative research program was then begun with the Texas Transportation Institute to investigate the specific cause of the cracking problem and determine what might be done to eliminate it. The Wave Equation method of pile driving analysis was used, in connection with data obtained from laboratory and field tests, to study the stresses that are developed in a pile during driving. The effects of driving accessories on the pile stresses were also studied by the wave equation method. Depending upon the particular type of hammer and pile used, the driving accessories may include any of the following items: (1) the ram and anvil of the hammer; (2) the capblock; (3) the helmet; (4) the cushion; and (5) the pile adapter. Changes in any of the accessories will have an affect on the pile stresses. The type of soil into which the pile is being driven will also have an affect on the pile stresses. All of the above items are accounted for in the wave equation analysis by using a discrete element, lumped-mass, spring and dashpot mathematical model. The engineering properties or the behavior characteristics of the driving accessories are commonly determined by reference to published "typical" or "average" values or by calculation from theoretical equations or formulas. While these methods usually provide values that are sufficiently accurate for

general use, the actual or "real" values are subject to variation on a pile-to-pile basis. The energy output of the hammer, the operating efficiency of the hammer, and the ram velocity at impact also have a profound influence on the driving operation but these quantities are quite often very difficult to determine with a high degree of accuracy. In spite of these problems, the wave equation is still an extremely useful tool with which to analyze the driving operation and it provides a means of obtaining valuable design data and construction control criteria.

It is necessary to simulate the hammer and driving accessories so that the force delivered to the pile can be calculated by a numerical procedure. Research with the wave equation method of pile driving analysis during the late 1960's and early 1970's showed that the accuracy of the method can be measurably improved if the force at the head of the pile can be determined by field measurement. The most accurate solution is obtained when the pile force is known for each instant of time that the force is doing useful work on the pile, generally for a time interval of 10 to 20 msec. In the early 1970's pile instrumentation technology had not advanced to the stage where this measurement could be made easily without the use of bulky, complex electronic equipment. The research indicated that the accuracy of the wave equation method could still be improved if only the peak force at the head of the pile could be determined. To achieve this measurement, a peak pile force readout unit was constructed by the Texas Transportation Institute. The instrument was designed to process an electrical signal incoming from a strain measurement circuit attached to the

pile. The installation of strain measuring devices to a pile usually requires the expenditure of time and the services of qualified technicians. To alleviate this problem, Research Study 2-5-76-31, "Development of a Transducer for Use in Measuring Peak Forces on Piles During Driving," was conducted.

Objective of the Study - - The objective of Study 2-5-76-31 was to develop a transducer for use with the Department of Highways and Transportation (DHT) readout instrument. The transducer to be developed was to be in the form of a strain gage system to be quickly and easily bonded to the exterior of piles, or a pair of transducers to be attached to the exterior of the pile, or in the form of a load cell to be placed on top of the pile. The study resulted in the design and construction of a load cell that is suitable for use on the top of square concrete piles up to 16-in. square. The study also demonstrated that commercially available strain gages encapsulated in plastic can be attached to the sides of concrete piles with a suitable epoxy to provide the required electrical signal for measurement of the peak force with the DHT readout unit.

This report describes the design, construction, and use of the load cell. It also presents data obtained from a field test at High Island, Texas, where the "glue-on" gages were used to measure the peak pile force. An example problem illustrating the application of the measured peak pile force in a wave equation analysis is given with the High Island test data being used for illustrative purposes.

PILE LOAD CELL

General Description - The load cell that was constructed to measure the peak force at the head of a pile is shown in Fig. 1. The load cell consists of three major component assemblies: (1) top member; (2) bottom member; and (3) flexural element member. The design drawings are given in Appendix III. All members were machined from 7075-T6 aluminum plates. The overall dimensions of the load cell are approximately 17-1/8-in. x 17-1/8-in. x 10-3/4-in. (435-mm x 435-mm x 273-mm), and the weight of the load cell, excluding the carrying case, is approximately 88 lb (392 N). The load cell was designed to be used on square concrete piles that do not exceed 16-in. per side.

The top member consists of a 16-5/8-in. x 16-5/8-in. x 5/8-in. (422-mm x 422-mm x 16-mm) aluminum plate with twelve 1/2-in. (13-mm) countersunk screw holes for rigidly attaching the top member to the flexural element member. Four 1/4-in. x 1.4-in. (6-mm x 36-mm) side plates are welded to the top member. The side plates have a 1/8-in. x 3/8-in. (3-mm x 10-mm) slot on the bottom side for inserting a continuous strip of rubber molding which provides a seal between the top member and bottom member. The seal prevents dust, moisture and other foreign elements from reaching the active surfaces of the flexural element member which is sandwiched between the top and bottom members, and protects the strain gage installation from damage due to environmental hazards.

The bottom member consists of a bottom plate and four bottom plate sides. The bottom plate contains nine 1/2-in. (13-mm) diameter countersunk holes which allow the bottom member to be securely attached to the

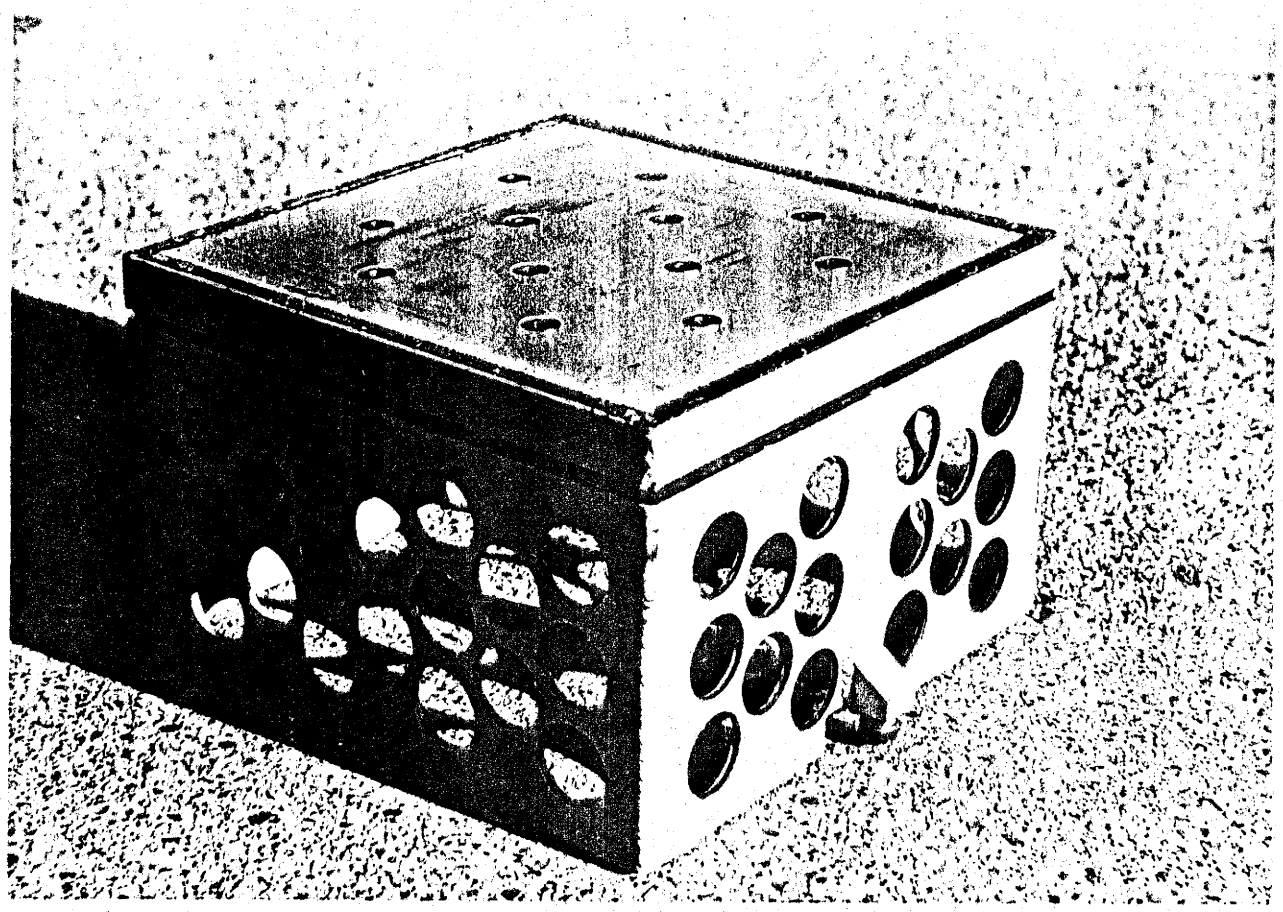

FIG. 1. - LOAD CELL FOR MEASURING DYNAMIC DRIVING FORCES ON THE TOP OF CONCRETE PILES.

flexural element member. The purpose of the bottom plate sides is to hold the load cell in place on the pile as the pile is being raised into position for driving, and also while the pile is being driven. The bottom plate sides have 2-in. (51-mm) diameter holes drilled to reduce the weight of the load cell. One of the bottom plate sides has a 1/8-in. (3-mm) diameter groove in which the leadwires from the strain gages are placed for routing to the point at which the wires are attached to the external connector mount. There is a 3/8-in. (10-mm) gap between the top side plates and bottom side plates which is closed by the rubber seal discussed above.

The flexural element member is the main element of the load cell for it is this member which contains the strain gage installation. The nominal dimensions of the flexural element member are 16-in. x 16-in. x 1.9-in. (406-mm x 406-mm x 48-mm). The member contains nine flexural elements, each element having four supports that are instrumented with strain gages. Each support has two strain gages attached, which gives a total of eight gages per flexural element, for a grand total of seventy-two strain gages in the entire load cell. The flexural elements are arranged in a 3 x 3 square grid pattern. The design of the flexural elements is discussed in the next section.

Design requirements - The flexural elements were designed in a manner such that the four bars that support the square interior block of each element are subjected to a state of pure shear at their midpoint when a load is applied to the load cell. Each of the four bars, or supports, act as a beam subjected to the shear and moment as shown in Fig. 2.

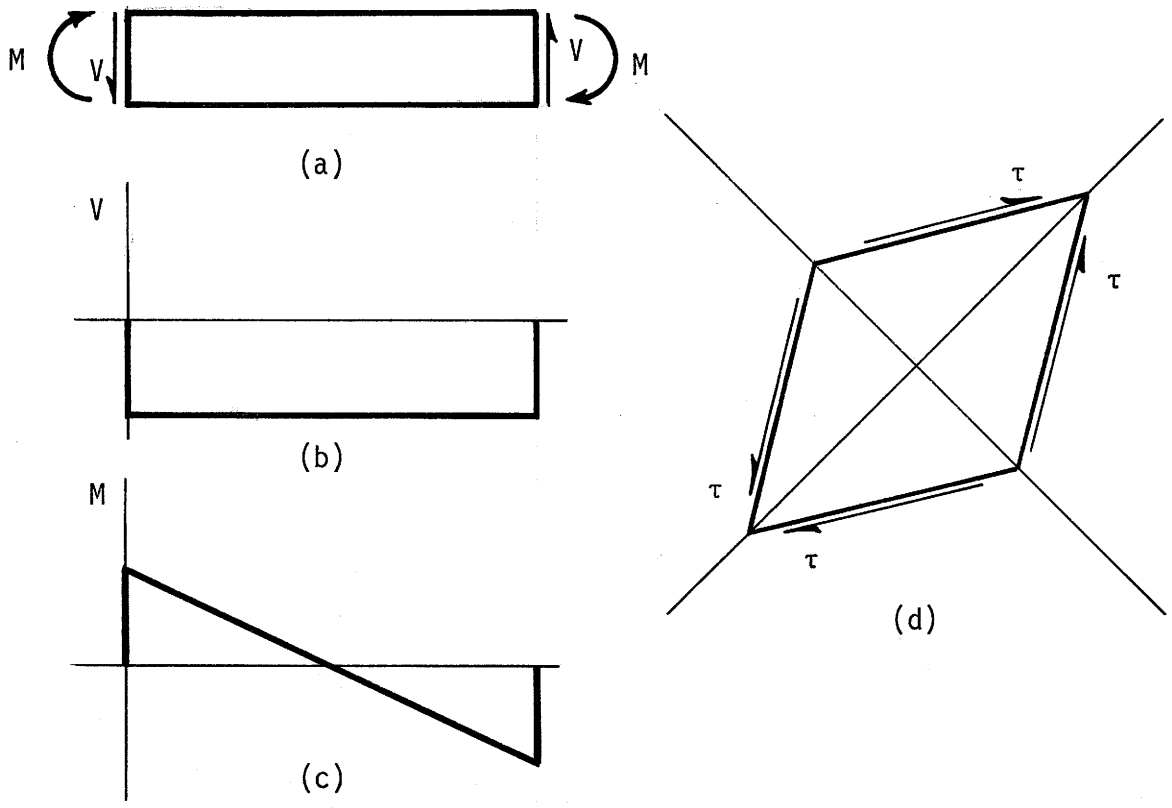

Fig. 2. Representation of the shear, moment and stress conditions for design of flexural element: (a) End shear and moment acting on the beam; (b) shear diagram; (c) moment diagram; (d) state of stress at a point in the middle of the beam.

The basic design equation that was used for sizing and proportioning of the supports was the shear stress equation (4)*

$$\tau = \frac{VQ}{It} \quad \ldots\ldots\ldots\ldots\ldots\ldots\ldots\ldots \quad (1)$$

in which τ = the shearing stress at a point in the beam; V = the shearing force in the beam at the point where the shearing stress is to be determined; Q = first moment about the neutral axis of that part of the cross-sectional area of the beam which lies above the plane in which the shearing stress is determined; I = moment of inertia of the

* Numbers in parentheses refer to the references listed in Appendix I.

beam about the neutral axis; and t = thickness of the beam. The material constants that were used in the design of the load cell were Young's modulus of elasticity E = 10.4 x 10^6 lb/in.^{2} (71.8 x 10^6 kN/m^2); modulus of rigidity G = 3.9 x 10^6 lb/in.^{2} (27 x 10^6 kN/m^2); and Poisson's ratio μ = 0.333. A single full-size flexural element was constructed before the fabrication of the prototype load cell was begun. The design drawing for the single element is presented in Fig. III-7 of Appendix III. The purpose of the test element was to determine the viability of the design concept and to ascertain the design modifications that were necessary prior to prototype construction.

The design load that was selected for the prototype was 750 kips (3340 kN). Assuming the load to be spread uniformly over a nominal 16-in. (406-mm) square area yields a stress of approximately 2900 lb/in.^{2} (20,000 kN/m^2). The largest driving stress on concrete piles usually does not exceed 2500 lb/in.^{2} (17,200 kN/m^2) which provides about a 15% margin of safety. The design of the flexural elements was based upon a "worst case" analysis, wherein the worst case is defined as the 750 kip (3340 kN) load being equally distributed over any three of the nine flexural elements. This situation is likely to arise when the hammer is extremely out of plumb or while driving batter piles, or whenever the hammer is delivering eccentric blows to the pile head.

As shown in Fig. 2 (c), the bending moment at the midpoint of the support is zero and a state of pure shear exists at that point. The support member has two strain gages attached, one gage on each side of the member. When subjected to a load the support member will tend to deform as indicated in Fig. 2(d). The deformation will consist of

compression in one direction and extension in the direction at 90° to the former. The axes of compression and extension are oriented at 45° with respect to the plane of the flexural element member. The strain gages are aligned in the direction of the compression and extension axes, consequently their output can be combined to increase the accuracy of the measured strain. The strain gages that were used to instrument the load cell were type EA-13-062AQ-350. Each gage has a resistance of 350.0 ± 0.15% ohms, and the gage factor is 2.11 ± 0.5% at 75°F (24°C). Each flexural element contains eight strain gages that constitute a single Wheatstone bridge. The nine individual bridges are wired in parallel, and the entire gage installation terminates in a four-wire harness that attaches to the interconnect cable through a multipin connector on the outside of the load cell (see Fig. 1 and Fig. III-2).

Evaluation Tests - After the prototype load cell was completed a series of laboratory tests were conducted to evaluate the linearity of the apparatus. The test series consisted of 5 centric loadings and 4 eccentric loadings. The 4 eccentric loadings were conducted in a manner that caused the resultant of the applied load to be offset from the center towards each of the four sides of the load cell. In all nine tests the load was applied in 10 kip (44 kN) increments up to a maximum of 300 kips (1330 kN). At each increment of load the strain in microinches per inch was recorded. For the five centric loadings the mean slope of the line representing the relationship between strain reading and applied load was 3.43 microin./in. per kip and the standard deviation was 0.026. For the four eccentric loadings the mean slope was 3.43 microin./in. per kip and the standard deviation

was 0.026.

In addition to the laboratory tests, it had also been planned to conduct one or more tests of the load cell in the field under actual driving conditions. A field test was set up to be conducted on some 16-in. (410-mm) square concrete piles that were being driven on the northwest freeway in Houston, Texas. Upon arriving at the test site it was discovered that the test could not be conducted because the pile helmet would not fit securely over the load cell. The problem was due to the fact that the contractor was using a pile helmet that was built for driving 18-in. (460-mm) piles but had been modified to drive 16-in. (410-mm) piles. Following the unsuccessful attempt in Houston it was not possible to schedule another field test.

Operational Procedure - The load cell was designed to be used in conjunction with the DHT peak force readout unit. The load cell is simply placed on top of the pile and connected to the readout unit by means of the interconnect cable that is provided with the load cell. Care must be taken during driving to ensure that the interconnect cable is held away from the pile to prevent the cable from being caught between the hammer or pile and the leads. Care must also be taken to ensure that the strain relief rope is attached to the interconnect cable to prevent the wires from being pulled loose inside the multipin connector. It is recommended that not more than 1/2-in. (13-mm) of plywood or other similar cushioning material be placed between the load cell and the pile to prevent the occurrence of extremely high contact stresses due to surface irregularities at the pile head.

The bridge excitation voltage is supplied directly from the readout unit. It is only necessary that the operator be familiar with

the calibration and operation procedures of the readout unit. These procedures are presented in detail in reference (4).

ALTERNATE TRANSDUCERS FOR CONCRETE PILES

Introduction - The Work Plan for this study included an evaluation of strain gages that are bonded to the exterior of piles. This method has recently been used to instrument steel piles that are used for offshore construction. Strain gages were welded to the pile sides, and the results obtained were very satisfactory. Prior to this study the method had not been tested on concrete piles. In order to adapt the method for use on concrete piles it was proposed that embedment type strain gages could be used. The embedment type gages had been used extensively in previous piling research, wherein the gages were attached to the steel prestressing strands. In order to determine whether or not the gages would work as well when attached to the exterior of concrete piles, a laboratory test and a field test were conducted.

Laboratory testing - A laboratory test was conducted to determine if the strain measured by embedment type gages attached to the exterior of a prismatic concrete test specimen would be the same as the strain measured by gages embedded inside the specimen. Four concrete specimens were cast for testing. The nominal dimensions of each specimen were 4-in. x 4-in. x 13-in. (100-mm x 100-mm x 330-mm). Each specimen was instrumented with 6 embedment type plastic encapsulated electric resistance strain gages. Two of the strain gages were embedded inside the test specimen; the four remaining strain gages were bonded to the exterior of the specimen. Two types of bonding agent were tested to determine whether or not there might be any difference between the strain measured externally and the strain measured internally due to the adhesive characteristics of the bonding agent used to mount the

exterior strain gages. Two of the external strain gages were bonded to the specimen with a "five-minute" rapid curing epoxy. The strain gages were placed 180° apart on opposite parallel faces of the specimens. The two remaining strain gages were mounted with an epoxy grout type adhesive that requires approximately 24 hr curing. The gages were mounted on the sides adjacent to those upon which the "five-minute" epoxy was used. The specimens were then tested in a dynamic repetitive loading machine. Fig. 3 shows one of the concrete specimens in place in the loading machine ready for testing. The strain gage on the left was bonded to the concrete with the "five-minute" epoxy; the strain gage on the right was affixed with the grout type adhesive. Note in Fig. 3 that the strain gages are attached in a position such that the active element (encased in plastic - not visible in the picture) is located in the center of the face of the concrete specimen.

The test procedure was to subject each specimen to a series of step input loading functions and measure the resulting strain indicated by the various strain gages. A step input function is a force pulse applied to the specimen in a manner such that the pulse rises almost instantaneously from zero to a preselected constant level of force at which it is held for a specific interval of time; at the end of the time interval the force is reduced almost instantaneously to zero and held there for a specified "waiting" period at the end of which the cycle repeats with the force again being instantaneously increased to its previous level. The pulse duration was approximately 30 msec for the tests described herein. The data were recorded on paper chart rolls for immediate visual inspection and evaluation, and in analog form on magnetic tape for later conversion to digital form for computer

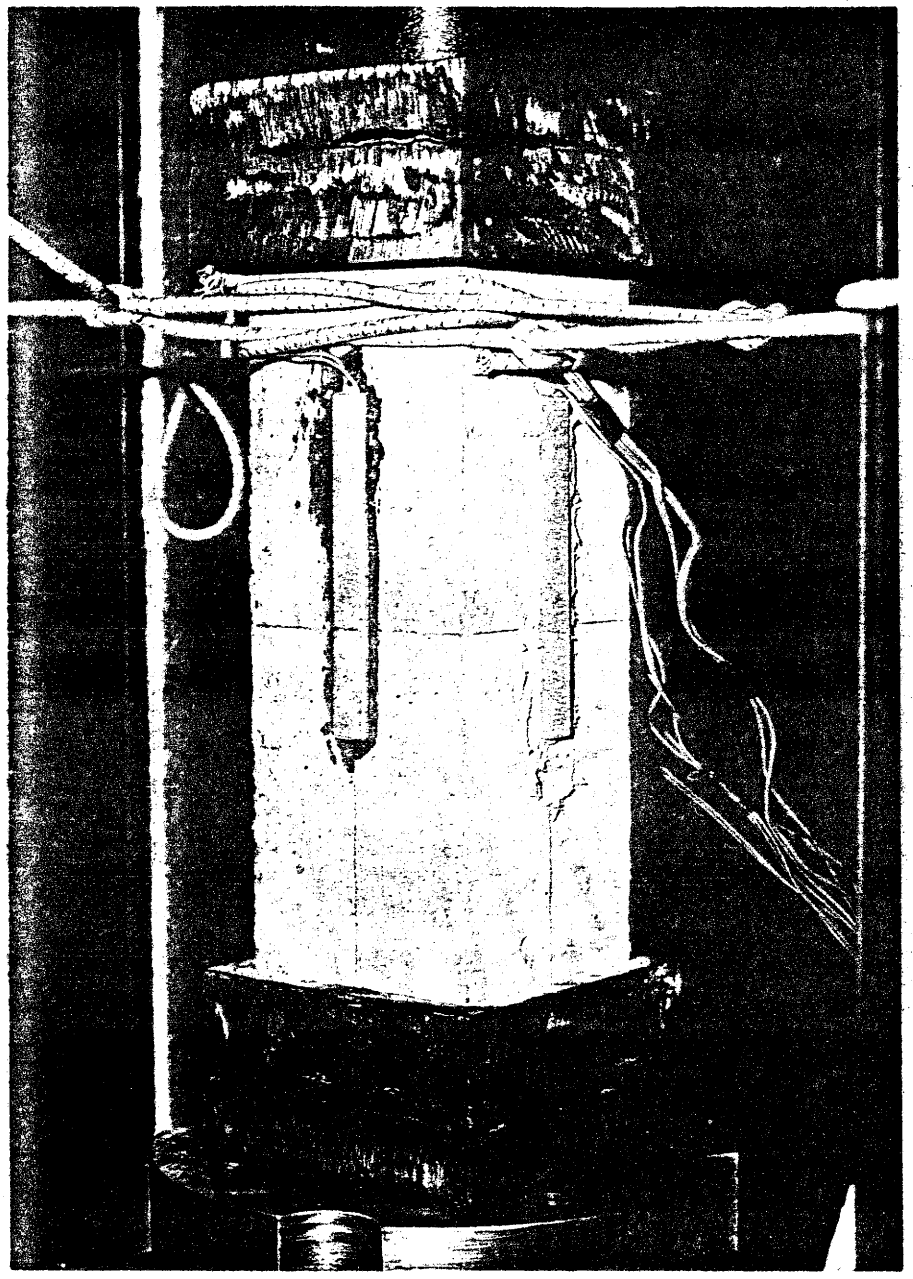

FIG. 3. - COMPRESSION TEST SETUP FOR COMPARING EXTERNAL TO INTERNAL STRAIN MEASUREMENTS AND EVALUATING BONDING EFFECTIVENESS OF TWO ADHESIVES.

processing and analysis. A series of 10 records, i.e., 10 gage excitations and responses due to 10 step input loadings, were obtained for each gage in or on the specimen. Prior to recording the 10 records per gage, the specimen was "cycled" with the step input being applied a sufficient number of times in order to "exercise" the strain gages and relieve any residual stresses that might otherwise have had an adverse affect on the data.

The data were analyzed by comparing the strain reading vs time records from the external gages to the strain vs time records from the internal gages. The implicit assumption in the analyses was that the internal strain readings were representative of the actual or true strain in the specimen, and were therefore used as the standard reference. The problem now at hand can be stated as: "Given the strain measured on an exterior surface of a body, predict or estimate the actual or "true" internal strain in the body." In order to do this there must be a known relationship or correspondence between the known and the desired quantities. The data analyses assumed that the internal strains were linearly related to the external strains and therefore could be expressed by the slope-intercept form of the equation of a straight line,

$$\varepsilon_i = a_o + a_1 \varepsilon_e \quad \ldots\ldots\ldots\ldots \quad (2)$$

in which ε_i = the internal strain; ε_e = the external strain; a_o = a constant which is numerically equal to the internal strain when the external strain is zero; and a_1 = slope of the straight line representing the correspondence between the internal and external strains. This relationship is shown graphically in Fig. 4.

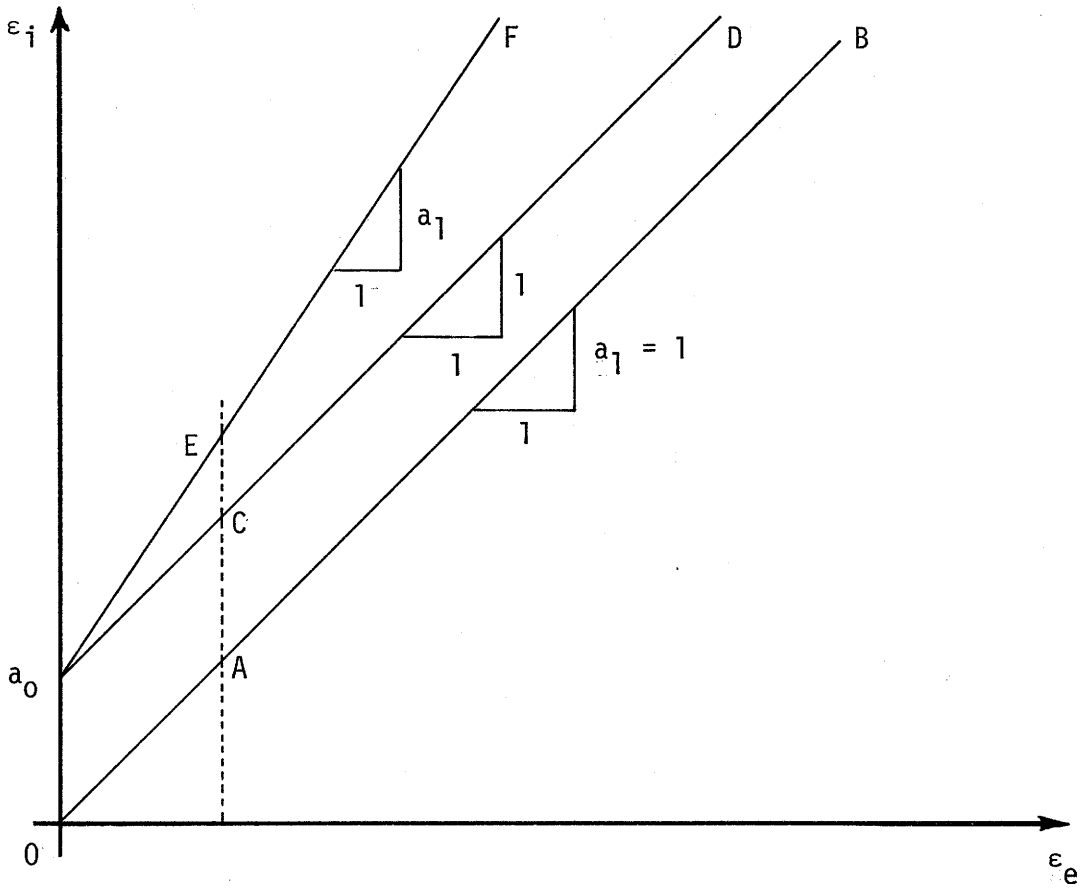

FIG. 4 - ILLUSTRATION OF THREE POSSIBLE STRAIGHT LINE RELATIONSHIPS BETWEEN INTERNAL STRAIN AND EXTERNAL STRAIN

In Fig. 4 $\overline{OAB}$ represents the conditions wherein there is an exact one-to-one correspondence between ε_i and ε_e, i.e., the internal strain is identical to the externally measured strain. Line $\overline{a_oCD}$ represents the case where there is still a one-to-one correspondence between the variables, however the dependent variable ε_i differs by some constant amount $a_o = \overline{AC}$. Finally, $\overline{a_oEF}$ represents the general case where there is no longer a one-to-one correspondence and the strains differ by some amount a_o initially when $\varepsilon_o = 0$. Fig. 4 shows that at low strain levels the constant "offset error" $a_o = \overline{AC}$ is more significant than the "slope error"

$\overline{CE}$. At large strain levels the "slope error" $\overline{CE}$ may be more significant than the "offset error."

A summary of the results obtained from the data analyses is given in Appendix V. Specimen 1 test results were noticeably different from the other three. For example, the average external strains were about 11% lower than the internal strains for specimen 1, whereas the external strains were larger for the other three specimens. If specimen 1 results are neglected the data do not show any dramatic effect due to the type of adhesive although it appears the grout type adhesive tended to show slightly higher strains when compared to the epoxy results.

Again neglecting specimen 1 results, the overall average values for the constants a_0 and a_1 of Eq. (2) were determined to be -2.42 micro-inches/inch and 0.980 respectively. These data appear to indicate that the "offset error" can be disregarded without serious consequence. If the "offset error" is neglected, making a correction for "slope error" alone, the error introduced may be as great as 6%. For practical applications this may be quite acceptable.

Full-scale field tests - Full-scale field tests were conducted to determine (1) if embedment type gages can be quickly and easily attached to the sides of concrete piles in the field; (2) if the field installation is adequate and rugged enough so that it will not sustain any damage during the process of pile handling and driving; and (3) if reliable data can be obtained from this type of instrumentation. The field tests were conducted on July 13, 1976 on State Highway 124 at the Intracoastal Canal north of High Island, Texas, in Chambers county. A 4300-ft (1300-m) long, 48-ft (15-m) wide bridge was being constructed at the test site to provide 73-ft (22-m) of minimum

vertical clearance over the Intracoastal Canal. The four test piles were located in bent 34 on the north side of the canal. Each test pile was 18-in. (460-mm) square and 55-ft (17-m) long. The piles were driven by a Delmag D46-02 hammer. The soil underlying the test site was predominantly a soft clay having an average liquid limit of about 62, an average plasticity index of about 40, and an average DHT Cone Penetrometer test N-value of about 14. The blow count was approximately 12 blows/ft (39 blows/m) for all four piles at final penetration. A static load test had been conducted earlier at bent 29, located 410 ft (125 m) south of bent 34. A maximum test load of 90 tons (800 kN) resulted in plunging failure of the pile on the day it was driven, November 10, 1975. The pile was again test loaded seven days later on November 17, 1975, at that time requiring a maximum of 160 tons (1420 kN) to cause a plunging failure. Boring logs, soil profiles, and pile test load data are given in the example wave equation problem in Appendix IV.

The pile instrumentation consisted of two PML-100S 300 ohm embedment type strain gages attached on opposite faces of the pile. Two additional PML-100S strain gages were required to complete the bridge; these two gages were located near the readout device. The strain gages were attached to the pile with 5-minute rapid setting two-part epoxy. The center of each gage was located in the center of the pile face, 54-in. (1.4-m) below the top of the pile. The strain gage leads were attached to an amphenol connector; the connector was fastened to a wooden block that was epoxied to the side of the pile. The wooden block served as a strain relief anchor for the connector cable between pile and readout.

Measurements of pile force and blows per 6-in. (150-mm) of pile penetration were taken as each pile was driven, with the blow count being recorded continuously throughout driving. Two modes of measurement were utilized for the pile force. The first was made with the peak-force readout unit that was constructed for DHT by TTI. Random readings were made until the pile was approximately 10-ft (3.0-m) from final penetration. Thereafter, readings were made for every third hammer blow, i.e., omitting two hammer blows between each reading, except for brief intervals when a hammer blow was recorded by means of the Honeywell Visicorder. The Visicorder was the second mode of measurement; it provided a continuous record of the force on the head of the pile with respect to time. The two modes were not independent as each received its activating signal from the same sensor. Theoretically the two modes should indicate the same peak force. In reality, the peak force measured by the Visicorder ranged from approximately 6% lower to 18% higher than corresponding values obtained with the DHT readout. These percentages are based on the average forces measured on the individual piles. There is no evident reason or explanation for this variation, however, the discrepancies are not excessive and are considered acceptable. The entire force records are given in Appendix IV along with the wave equation example problem.

The testing that was done at High Island was not specified in the project plans. Consequently it had to be done in a manner that would cause virtually little or no delay or hinderance to the contractor's forces. As an indirect consequence, two factors which are extremely important in the analysis of the data were beyond control of those involved with the research study. The first concerns the location of

the pile test load; the second concerns the pile modulus of elasticity. A brief discussion of the general nature of the problems involved is presented here; details concerning the affects of these factors is given in Appendix IV - Example Wave Equation Problem Illustrating Utilization of High Island Field Test Data.

Ideally, the instrumented pile tests should have been conducted at the pile test load location. This was not the case as the two tests were located over 400 ft (122 m) apart. Examination of the soil profiles at bents 29 and 34 seem to indicate no significant differences in soil conditions at the two locations. However, the blow counts at final penetration during initial installation differed by an approximate factor of two (6 blows/ft (20 blows/m) at bent 29 vs. 12 blows/ft (39 blows/m) at bent 34). In view of these similarities and differences, there is no sound assurance that: (1) the hammer force vs time record at bent 29 would have been the same as at bent 34 if the instrumented tests had been conducted at bent 29; and (2) the pile test load results at bent 34 would have been the same as at bent 29 if the static test load had been conducted at bent 34. Consequently there is not much reason to expect a wave equation bearing graph that is computed from data obtained at bent 34 to accurately predict the static bearing capacity at bent 29 from driving data measured at bent 29.

The problems arising from the second factor, viz. the modulus of the concrete pile, stem from the fact that a force in the pile cannot be measured directly. Instead, the force must be deduced from the strain in the pile which can be measured directly. The force in the pile can be found by computing the product of pile cross-section

area, pile strain, and modulus of elasticity. Ordinarily the modulus of elasticity is determined from tests on standard 6.0-in. x 12.0-in. (152-mm x 305-mm) concrete cylinders cast from the same mix as the pile. It was not possible to do this in connection with the High Island tests as the piles were cast long before the tests took place. Consequently, there is a degree of uncertainty associated with the actual magnitude of the pile force; in consideration of typical values for the modulus of elasticity of concrete, this degree of uncertainty is on the order of 60%. A more complete discussion, together with numerical data, is given in Appendix IV.

CONCLUSIONS AND RECOMMENDATIONS

Conclusions - A portable load cell for measuring dynamic forces on the head of a driven pile was designed and constructed for use on square concrete piles. An alternate method for measuring the pile force, utilizing expendable strain gages that are rigidly attached to the pile, was tested in the laboratory and in the field. On the basis of data obtained and experience gained throughout the course of this research study, the following conclusions are made:

1. The design and construction of a load cell for measuring pile driving forces is both an art and a science. It is primarily an art because it requires the use of unlimited creative ability and imagination to overcome the many vexing problems associated with the task. It is to a lesser extent a science because it necessarily must draw upon the knowledge gained by individuals who have become keenly aware of the variables and factors involved in piling behavior, wave propagation, wave mechanics and engineering measurements through study and experience. It is a project that should not be left to the beginner or the inexperienced who lack the proper training, background and understanding in the areas of civil, electrical and mechanical design and engineering and product fabrication.
2. The design of a single "universal" load cell for use on all types and sizes of piling is at best a formidable task; several designs based on pile type may be a more realistic objective.
3. The use of expendable strain gages rigidly attached to a pile can be relied upon to provide accurate data, provided that the necessary

precautions concerning gage application and careful pile handling are observed.

4. The necessity of determining reasonably accurate values for all of the important variables and parameters affecting the measurement of pile forces must not be overlooked. The lack of one vital piece of information can negate the results of the most carefully executed test program.

Recommendations - Throughout the course of this research study, and as a result of some of the work that was done, several ideas or points of interest emerged that might be helpful in any future studies that are conducted in this particular area of research or hardware development. Therefore the following recommendations are offered as an aid and a guide to those who will continue on to advance the technological level achieved during this study.

1. It is recommended that field tests of the present load cell be conducted whenever possible. These tests should be directed not only towards establishing the merit of the present system but also to isolating or identifying the weak points or problem areas, of which there are many. Potential problem areas may encompass actual field use of the load cell, including handling, operation and personnel familiarization and training; adaptation of the load cell to fit the many and varied makes and models of hammers and driving accessories; and fundamental deficiencies in the design of the load cell, including both the mechanical construction and the active sensing elements regardless of their type (i.e., electrical, mechanical, or other).

2. It is recommended that concrete cylinders be cast when measurements are to be made on concrete piles. The cylinders should then be tested to determine the modulus of elasticity of the concrete as this value is required in order to compute the load in the pile from the measured strain ($P = AE\varepsilon$), and also to compute the stiffness ($K = AE/L$) of pile sections for wave equation analyses.

APPENDIX I. - REFERENCES

1. Coyle, H.M., Bartoskewitz, R.E., and Berger, W.J., "Bearing Capacity Prediction by Wave Equation Analysis - State of the Art," Research Report 125-8F, Texas Transportation Institute, Texas A&M University, College Station, Texas, August, 1973.

2. Kaiser, F.X., Jr., Coyle, H.M., Milberger, L.J., and Bartoskewitz, R.E., "The Measurement of Pile Driving Forces and Its Application to Wave Equation Analysis of Piles," Research Report 195-1F, Texas Transportation Institute, Texas A&M University, College Station, Texas, September, 1975.

3. Lowery, L.L., Jr., Hirsch, T.J., Edwards, T.C., Coyle, H.M., and Samson, C.H., Jr., "Pile Driving Analysis - State of the Art," Research Report 33-13F, Texas Transportation Institute, Texas A&M University, College Station, Texas, January, 1969.

4. Milberger, L.J., and Zimmer, R.A., "Operating Instructions for Dynamic Pile Force Readout, Model 2174," Research Report 174-1F, Texas Transportation Institute, Texas A&M University, College Station, Texas, August, 1974.

5. Miller, F.E., and Doeringsfeld, H.A., Mechanics of Materials, 2nd edition, International Textbook Company, Scranton, Pennsylvania, 1955.

APPENDIX II. - NOTATION

The following symbols are used in this report:

A = cross-sectional area;

a_o = regression coefficient equal to the intercept of a straight line with the vertical axis;

a_1 = regression coefficient equal to the slope of a straight line;

cal R = value of the calibration resistor to be used when calibrating the DHT peak force readout unit;

E_{conc} = Young's modulus of elasticity for concrete pile;

e = coefficient of restitution;

eff = operating efficiency of diesel pile driving hammer;

GF = $(\Delta R/R)/(\Delta L/L)$ = dimensionless gage factor of electric resistance strain gages;

g = acceleration due to gravity = 32.2 feet per second per second;

h = height of fall (stroke) of the ram in a pile driving hammer;

I = moment of inertia;

J = damping constant of soil beneath the point of a pile;

J' = damping constant of soil along the side of a pile (friction damping constant);

K = stiffness or spring constant of a pile section = AE/L;

L = length of a pile section;

N_{eff} = number of effective longitudinal gages in a strain gage Wheatstone bridge;

P = calculated value of load or force represented by the simulated strain when calibrating the DHT peak force readout unit;

Q = first moment about the neutral axis of that part of the cross-sectional area of a beam which lies above the plane in which the shearing stress is determined, Eq. (1); or soil quake in friction along the side of a pile, equal to maximum elastic soil deformation before plastic soil failure occurs, Fig. IV-9;

Q_p = soil quake beneath the point of a pile;

R = strain gage resistance;

R_l = leadwire resistance, or resistance of interconnect cable;

t = thickness of a beam at the point where the shearing stress is determined;

V = shearing force in a beam at the point where the shearing stress is determined;

v = velocity of the ram of the pile driving hammer at impact;

W = weight of hammer or pile segment used in the wave equation method of pile driving analysis;

γ = explosive force between ram and anvil; parameter which specifies ability of a spring to transmit tension forces;

∇ = symbol denoting a change in the value of a variable;

ε = engineering strain;

τ = shearing stress.

APPENDIX III. - LOAD CELL MACHINE DRAWINGS

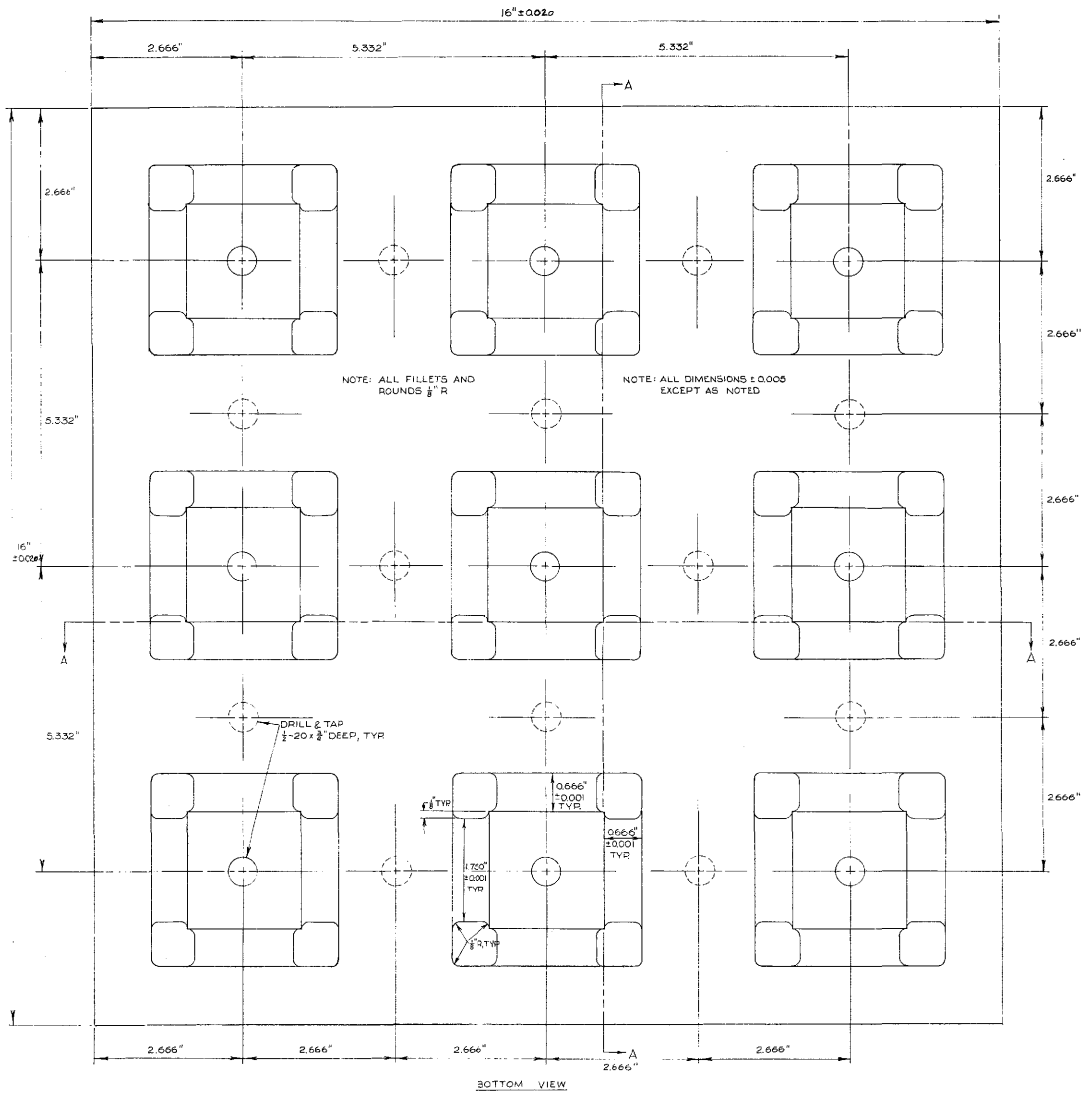

BOTTOM VIEW

FLEXURAL ELEMENT MEMBER

MACHINE FROM 2" BLOCK 7075-T6 ALUMINUM

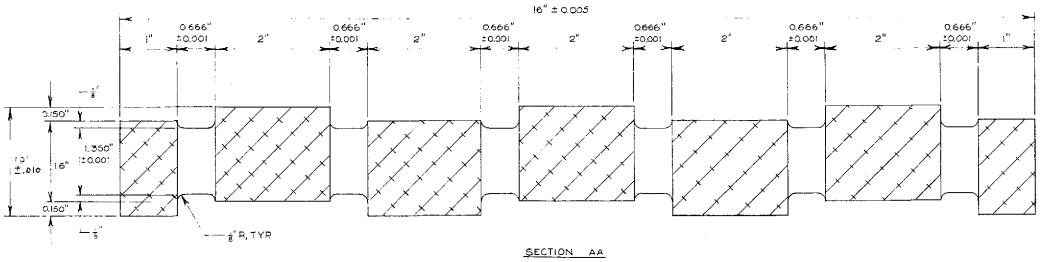

SECTION AA

TEXAS A&M UNIVERSITY				
REVISIONS			TEXAS TRANSPORTATION INSTITUTE COLLEGE STATION, TEXAS 77843	
NO.	DATE	BY		
1.				
2.				
3.				
4.				
5.				
PROJECT NO. 2031	DATE 15 JAN 76	DRAWN BY Mark	SCALE NONE	
TITLE CONCRETE PILE TRANSDUCER			SHEET NO. 1 OF	

FIG. III-1. - FLEXURAL ELEMENT MEMBER

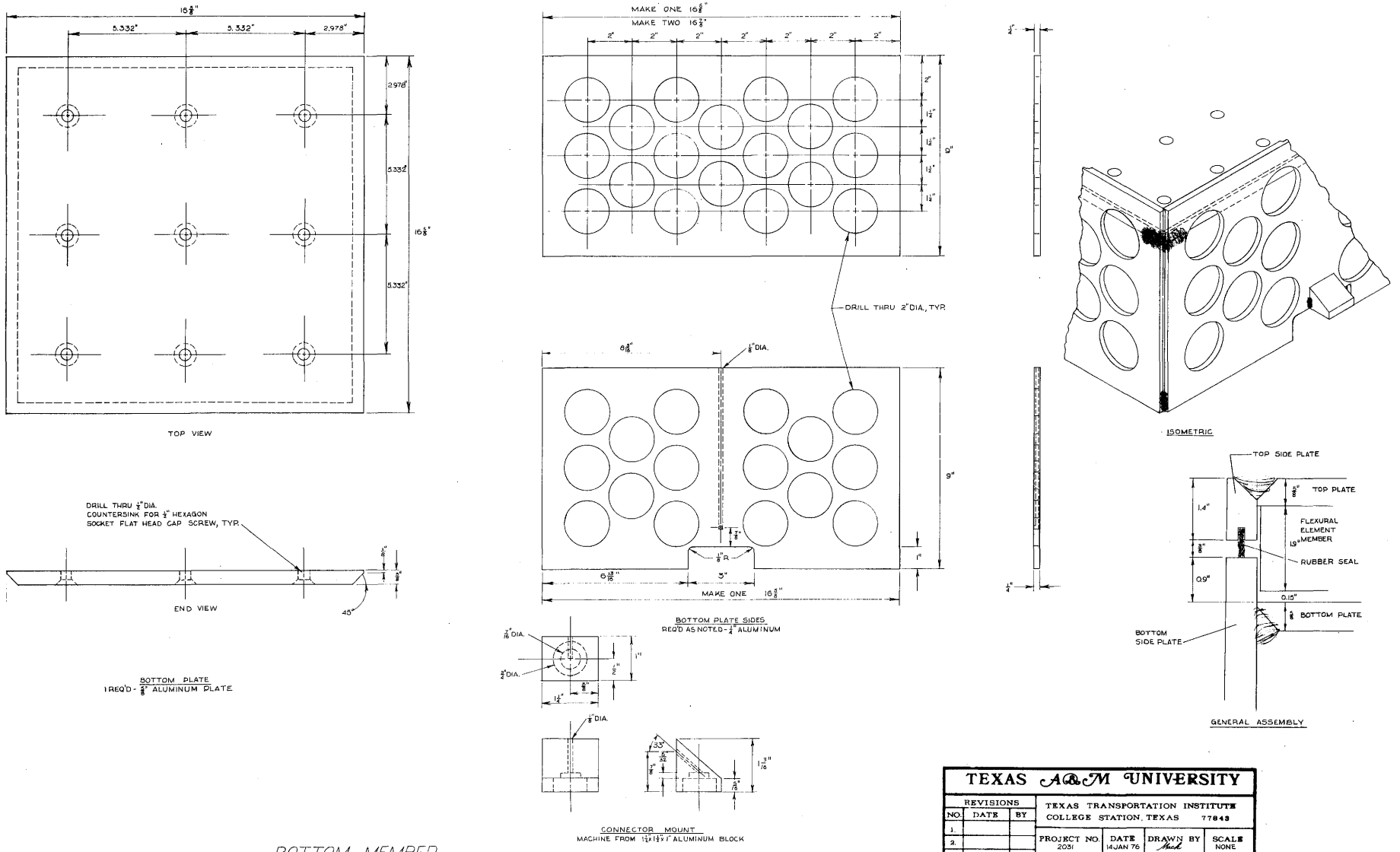

BOTTOM MEMBER

MACHINE FROM ALUMINUM PLATE AS NOTED

TEXAS A&M UNIVERSITY					
REVISIONS			TEXAS TRANSPORTATION INSTITUTE COLLEGE STATION, TEXAS 77843		
NO.	DATE	BY	PROJECT NO. 2031	DATE 14JAN 76	DRAWN BY Mack	SCALE NONE
1.			TITLE: CONCRETE PILE TRANSDUCER		SHEET NO. 2 OF
2.					
3.					
4.					
5.					

FIG. III-2. - BOTTOM MEMBER

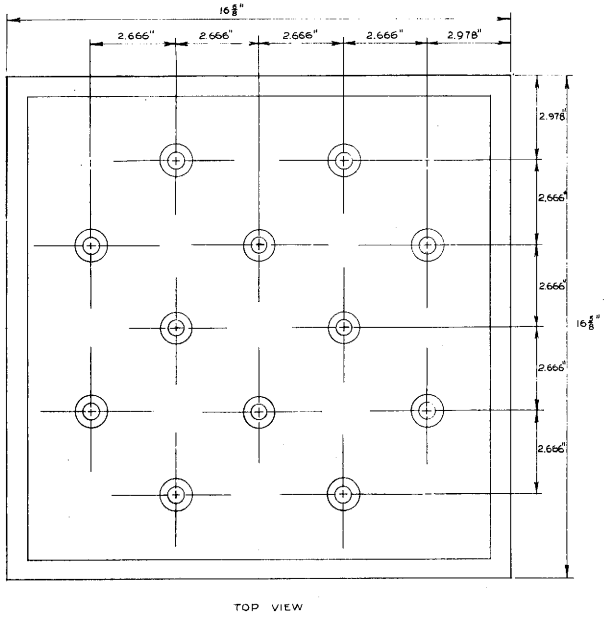

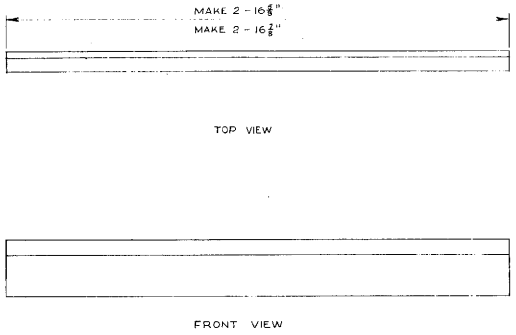

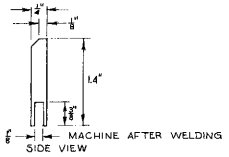

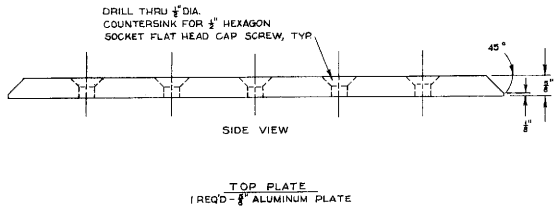

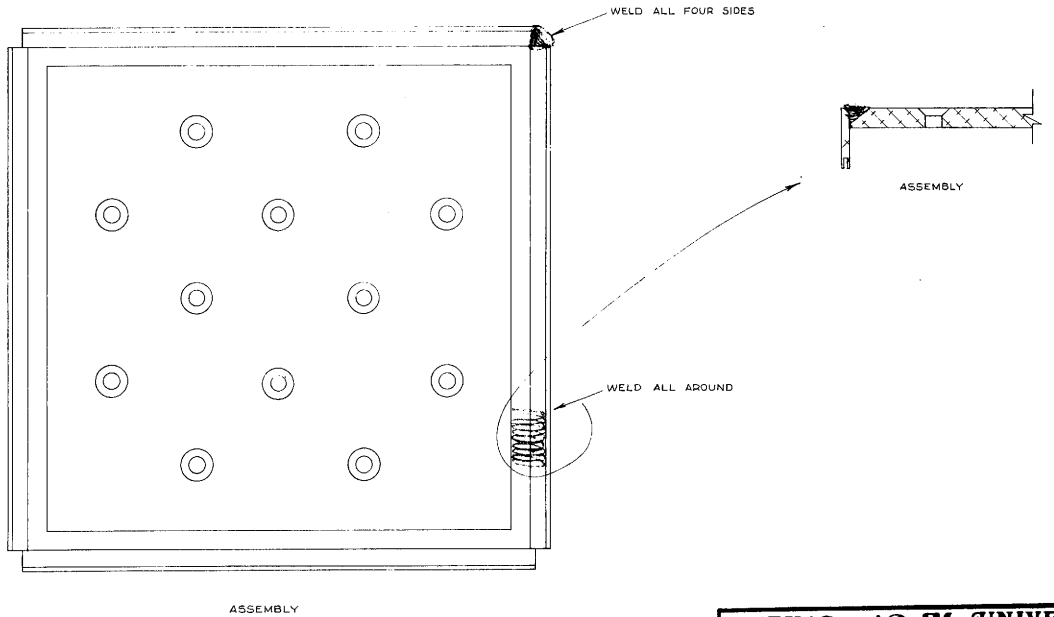

TOP MEMBER
MACHINE FROM ALUMINUM PLATE AS NOTED

TEXAS A&M UNIVERSITY					
REVISIONS			TEXAS TRANSPORTATION INSTITUTE COLLEGE STATION, TEXAS 77843		
NO.	DATE	BY	PROJECT NO. 2031	DATE 19JAN 76	DRAWN BY Mack	SCALE NONE
1			TITLE CONCRETE PILE TRANSDUCER			SHEET NO. 3 OF
2						
3						
4						
5						

FIG. III-3. - TOP MEMBER

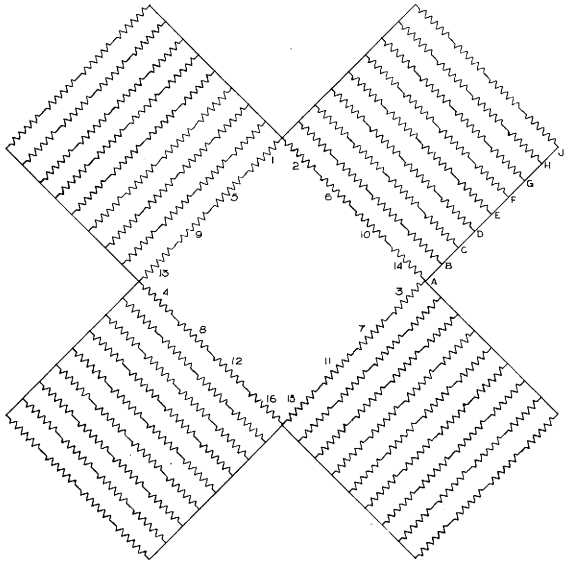

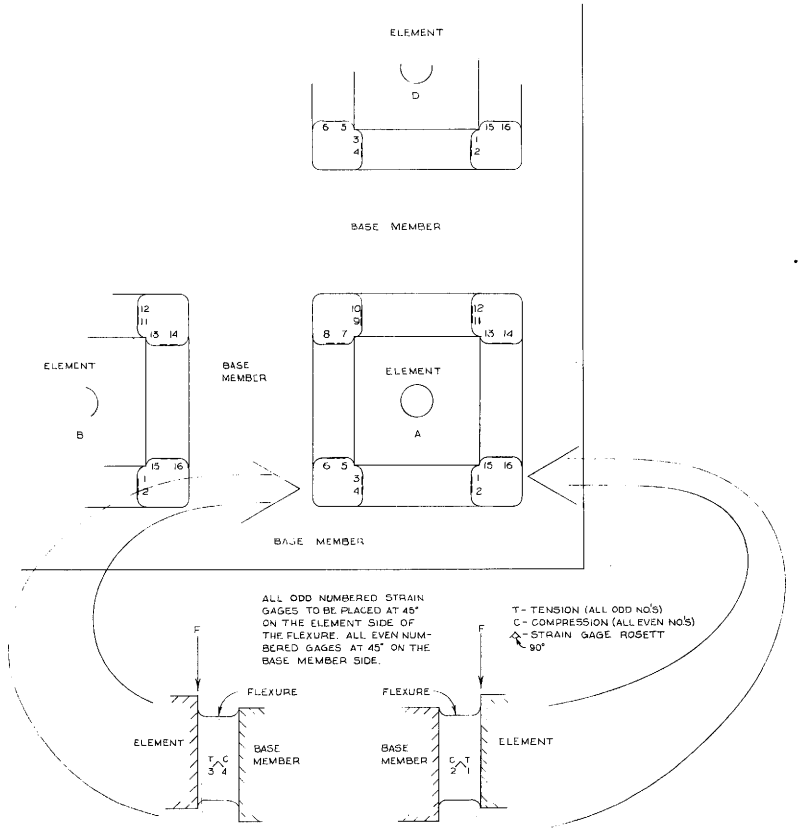

STRAIN GAGE PLACEMENT

STRAIN GAGE NO. EA-13-062TV-350 Ω

TEXAS A&M UNIVERSITY					
REVISIONS			TEXAS TRANSPORTATION INSTITUTE COLLEGE STATION, TEXAS 77843		
NO.	DATE	BY			
1.			PROJECT NO. 2031	DATE 26 JAN 76	DRAWN BY Mark	SCALE N/A
2.						
3.						
4.			TITLE CONCRETE PILE TRANSDUCER		SHEET NO. 4 OF
5.					

FIG. III-4.- STRAIN GAGE PLACEMENT

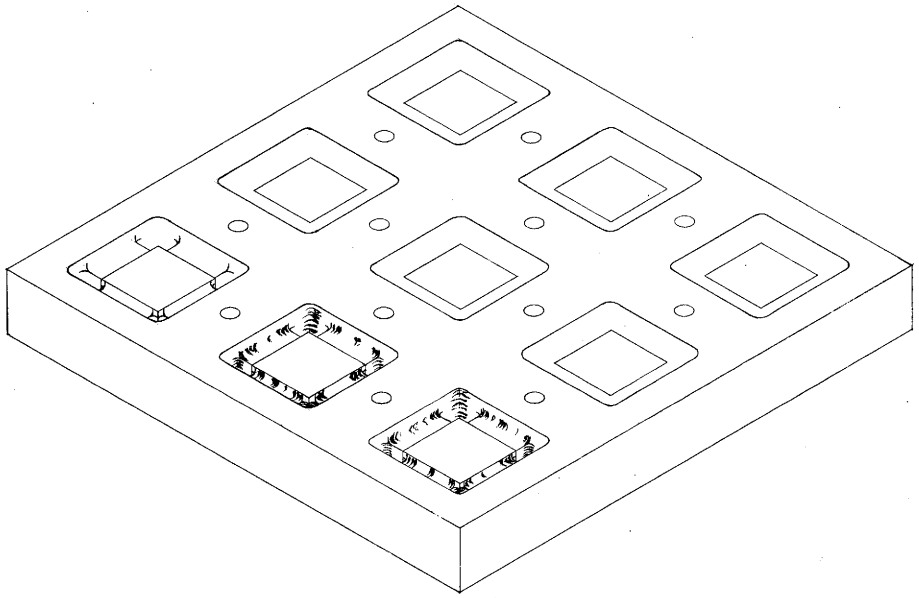

TOP VIEW

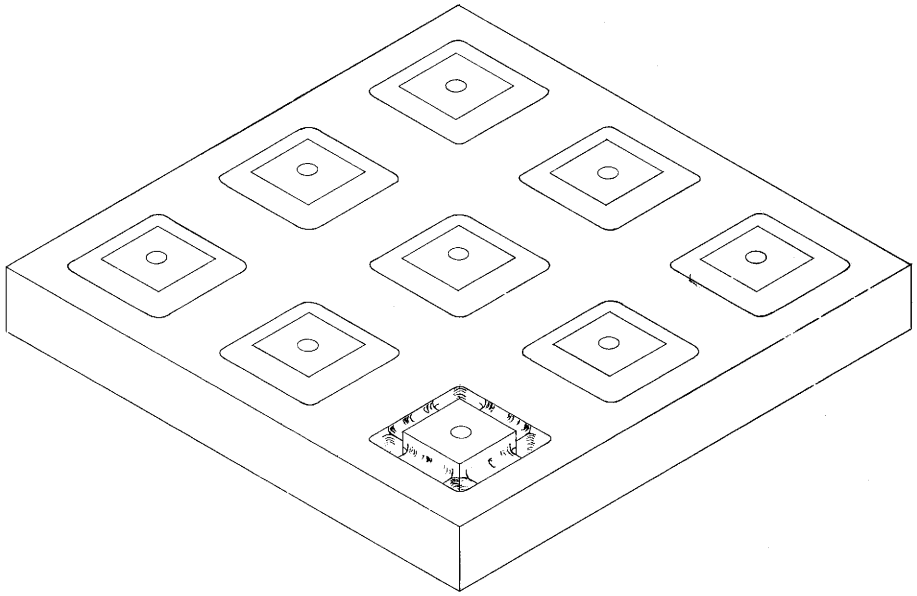

BOTTOM VIEW

TEXAS A&M UNIVERSITY					
REVISIONS			TEXAS TRANSPORTATION INSTITUTE COLLEGE STATION, TEXAS 77843		
NO.	DATE	BY			
1.			PROJECT NO. 2031	DATE 14 JAN 76	DRAWN BY Mark	SCALE NONE
2.						
3.			TITLE CONCRETE PILE TRANSDUCER		SHEET NO. 5 OF
4.					
5.					

FIG. III-5. - ISOMETRIC VIEW OF FLEXURAL ELEMENT MEMBER

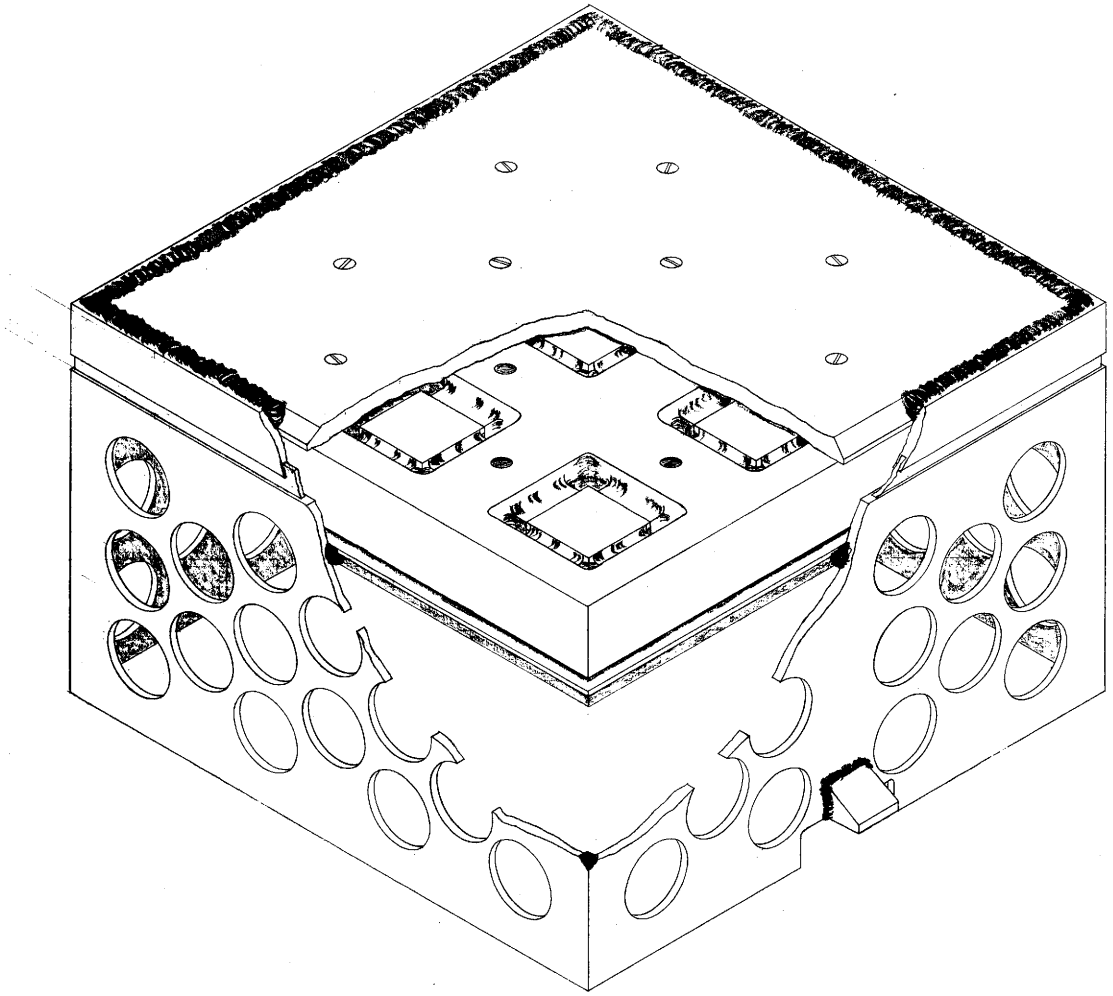

ASSEMBLY

TEXAS A&M UNIVERSITY					
REVISIONS			TEXAS TRANSPORTATION INSTITUTE		
NO.	DATE	BY	COLLEGE STATION, TEXAS 77843		
1.			PROJECT NO. 2031	DATE 2 FEB 76	DRAWN BY Mack	SCALE NONE
2.						
3.			TITLE		SHEET NO.
4.			CONCRETE PILE TRANSDUCER		6 OF
5.					

FIG. III-6. - LOAD CELL ASSEMBLY

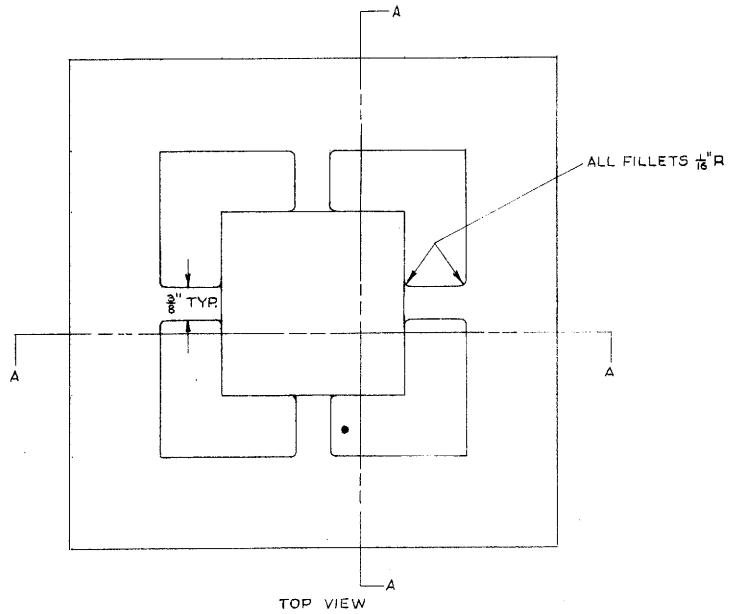

TOP VIEW

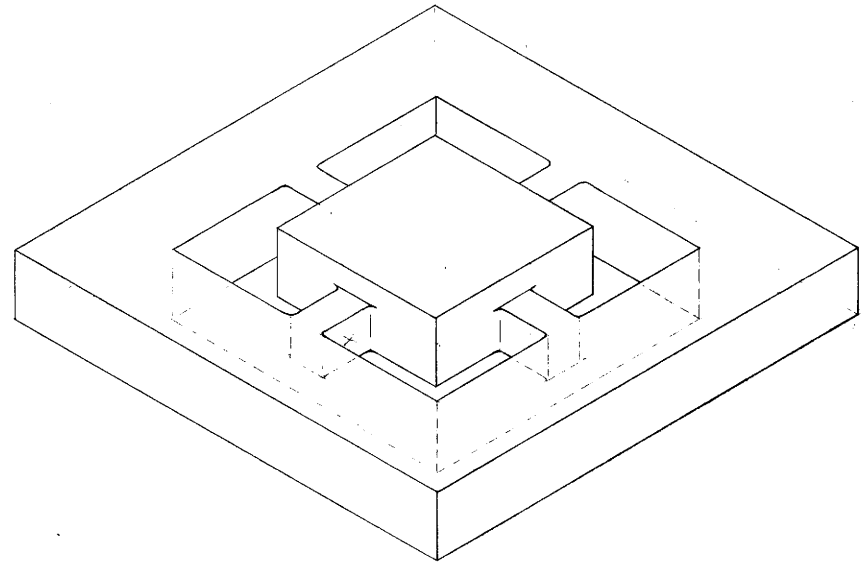

PILE TRANSDUCER
TEST MODEL
MACHINE FROM 1" ALUMINUM PLATE

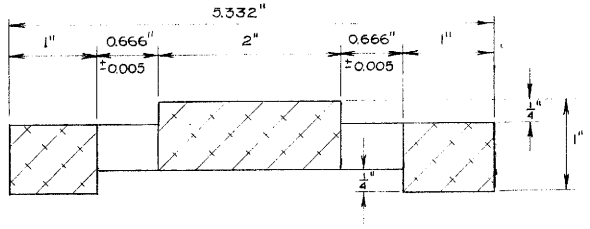

SECTION AA

TAMU-TTI
9 JANUARY 1976
3258
Mack

FIG. III-7. - FLEXURAL ELEMENT TEST MODEL

APPENDIX IV - EXAMPLE WAVE EQUATION PROBLEM ILLUSTRATING UTILIZATION OF HIGH ISLAND FIELD TEST DATA

Introduction - The purpose of Appendix IV is to illustrate the use of the wave equation method as it applies to pile driving. Specifically, this appendix is intended to illustrate how the measured forces at the head of a pile are used with the wave equation method, particularly with regard to developing a bearing graph for prediction of bearing capacity.

General information regarding the location of the High Island test site and the nature of the work being conducted there was given in the main text of this report in the section on "ALTERNATE TRANSDUCERS FOR CONCRETE PILES." Contained in this appendix will be the detailed data consisting of boring logs, driving records, and pile force measurements along with the presentation of the data analyses and results.

Soil Data - Figs. IV-1 through IV-3 present the drilling logs for hole no's. 3 through 5 respectively. The test holes were drilled by DHT crews during March and April, 1971. Hole 3 is located approximately 100 ft northeast of bent 34 which is the bent in which the instrumented piles were driven; hole 4 is located approximately 110 ft south of bent 34. Hole 5 is located 31 ft to the right of bent 29 where the test loads were conducted. At bent 34 an excavation was made to an average depth of 3.47 ft below natural ground. The tops of the 55-ft piles were driven to within one ft of the bottom of the excavation, thereby placing the point of the piles approximately 57.5- to 58.5-ft below original ground. The boring logs indicate CL soils at this depth, having liquid limits of 39% and 31% and plasticity indices of 20% and 12% at holes 3 and 4 respectively. The DHT cone penetrometer test values

DISTRICT 20 COUNTY Chambers HIGHWAY SH-124
HOLE Nº 3 STATION 192+84 GROUND ELEV. 3.6
LOC. FROM CENTERLINE 40' Rt.

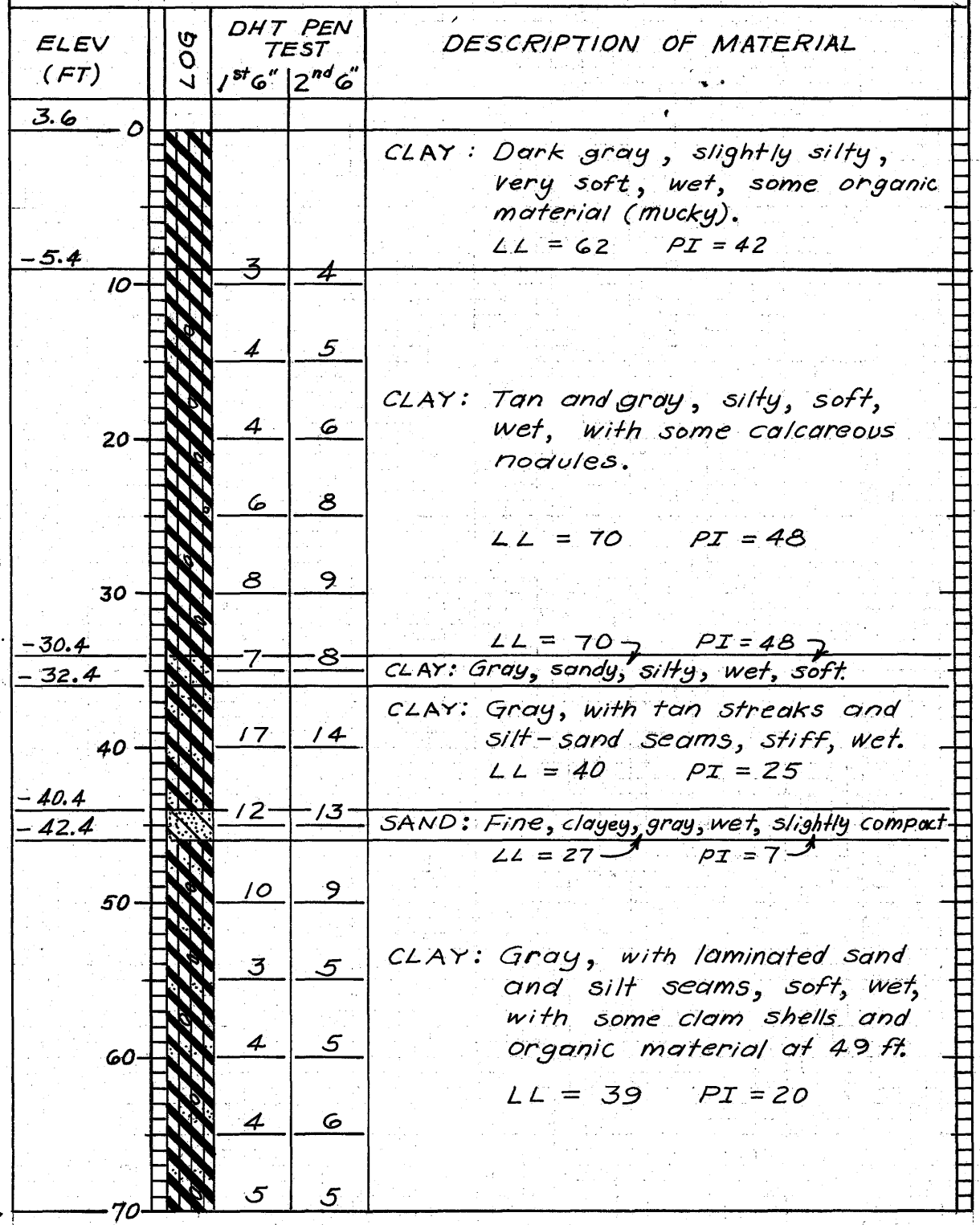

FIG. IV-1. – BORING LOG OF TEST HOLE Nº. 3 LOCATED APPROXIMATELY 100 FT NORTHEAST OF BENT 34.

DISTRICT 20 COUNTY Chambers HIGHWAY SH - 124
HOLE No. 4 STATION 190 + 89 GROUND ELEV. 2.8
LOC. FROM CENTERLINE 32' Rt

ELEV (FT)	LOG	DHT PEN TEST 1st 6"	DHT PEN TEST 2nd 6"	DESCRIPTION OF MATERIAL
2.8				
0				
		4	4	CLAY: Tan and gray, silty, soft and wet.
10		5	5	
-14.2				
		6	7	Depth 0'—39': LL = 81 PI = 56
20		7	7	
		7	8	CLAY: Tan and gray, silty, soft and wet with some calcareous nodules.
30		8	9	
-36.2				
		10	8	
40				SAND: Fine-grained, silty, clayey, gray, laminated with 1/4" strata, soft. LL = 29 PI = 9
-42.2		5	4	
		6	5	CLAY: silty, sandy, "mucky," soft, gray.
50		3	4	LL = 31 PI = 12
-57.2		4	5	
60				
		5	6	CLAY: With 1/8" silt lamina, gray, soft, wet, some organic matter.
70		4	4	LL = 78 PI = 53

FIG. IV - 2. — BORING LOG OF TEST HOLE No. 4 LOCATED APPROXIMATELY 110 FT SOUTH OF BENT 34

DISTRICT 20 COUNTY Chambers HIGHWAY SH - 124
HOLE No. 5 STATION 187+84 GROUND ELEV. 2.7
LOC. FROM CENTERLINE 31' Rt

ELEV (FT)		SOIL	DHT PEN TEST 1st 6"	2nd 6"	DESCRIPTION OF MATERIAL
2.7	0				CLAY: Dark gray, slightly silty, very soft, wet, some organic matter. LL = 84 PI = 56
-5.3					
	10		3	4	
			4	5	CLAY: Tan and gray, silty, soft, wet. Some calcareous nodules from 19 – 20'.
	20		6	8	LL = 66 PI = 46
			7	8	
			7	9	
-29.3	30				
			4	4	CLAY: Gray, with tan streaks, also with silt strata, wet, soft. LL = 58 PI = 39
-36.3			6	11	
-39.3	40				SAND: Fine grain, Silty, gray, clayey, wet, loose. LL = 27 PI = 6
			3	4	
			3	3	CLAY: Gray with sand strata, some clam shells at 44', wet, very soft.
	50				LL = 43 PI = 24
-53.3			3	4	
	60		4	5	CLAY: Gray, with some silt seams, wet, soft.
			4	6	LL = 71 PI = 45
			4	5	
	70				

FIG. IV - 3. — BORING LOG OF HOLE No. 5 LOCATED APPROXIMATELY 31 FT RIGHT OF BENT 29

average about 8 blows per foot, indicative of a soft consistency soil. Consequently it is logical to expect that the pile would be essentially a "friction" pile having probably not more than 20% of the load carried by end-bearing during initial driving and load testing. Therefore 20% was selected as the ratio of point load to total load for the wave equation analysis. The boring logs also show that the soil from the surface to the pile tip is predominantly a soft silty clay. Therefore the soil damping parameters to be used in the wave equation are the clay parameters given in (1), i.e., $Q_s = Q_p = 0.1$-in., J' = 0.2-sec per ft and J = 0.01-sec per ft.

Hammer Data and Driving Records - The hammer that was used to drive the piles at bents 29 and 34 was a Delmag D46-02 single-acting diesel hammer. The hammer has a 10,100-lb (4,580-kg) ram, a 1,980-lb (898-kg) anvil, and a 10-ft 8-3/4 in. (3.27-m) maximum stroke. The manufacturer's maximum energy rating for the hammer is 105,000 ft-lb (142,000 N-m). The D46-02 has a four-position pumpsetting which allows the operator to select either 46%, 64%, 86%, or 100% of maximum rated energy output. While driving the instrumented piles at bent 34 the hammer was throttled to its lowest energy output.

The capblock consisted of 4 layers of 3/4-in. (19-mm) pine plywood, 23-in. (580-mm) square. The cushion was made from 3 layers of 2-in. (51-mm) green oak with the grain horizontal. The cushion was an irregular-shaped octagon having parallel faces spaced 24-, 22-, 24- and 23-in. (610-, 560-, 610- and 580-mm) apart; the net area of the cushion was calculated to be 440-in.^{2} (0.29-m^2). To calculate the AE/L stiffness for the capblock and cushion, the elastic modulus for pine plywood and green oak were taken as 25,000 psi (170,000 kn/m^2) and 45,000 psi

(310,000 kn/m^2) respectively. These values yielded stiffness values of 3200 kips/in. (560,000 kn/m^2) and 3300 kips/in. (580,000 kn/m^2) for the capblock and cushion, respectively. The pile helmet weighed 1750-lb (794-kg). The calculated stiffness values were computed on the basis of moduli of elasticity values taken from (2), but the combined stiffnesses of the cushion and the first pile segment has to be reduced, as will be explained in more detail in a subsequent section, in order to achieve a reasonable value for the peak pile top force as computed by the wave equation.

The driving record of the test load pile at bent 29 is given in Table IV-1. The driving record of the four instrumented piles that were driven at bent 34 are given in Figs. IV-4 and IV-5. These records indicate the number of hammer blows per foot of pile penetration and the stroke of the hammer at various penetration depths. Note that there are no data given for pile penetrations from the surface down to approximately 20 ft (6.1 m). This is because the piles sank 10- to 15-ft (3.0- to 4.6-m) under their own weight and the additional penetration to the point where the records begin was achieved during the process of dropping the ram while attempting to start the hammer. The soil bearing capacity was so low, and the ram fall height and pile penetration per drop of the ram were so uncertain, as to render any blow count during this period almost worthless.

Fig. IV-6 is a plan view of the excavation, footings and piles at bent 34, indicating the lettering scheme that is used to identify the footings and piles in the text of this report. The footings are lettered A, B, and C from west to east; the piles in each footing are designated A through E from south to north and from west to east.

Bent #29 23-58 Bent 29(DTL)

Texas Highway Department
Form 181 2-57-5m

TEST PILE DATA

Test Pile No. 4

County Chambers Project BRF 749(6) Highway No. 124 Control 367-2-48

Structure or Stream Intracoastal Canal Sta. *187+84 Rt. 9 Ft. Design Brg. Resist. 60 Tons

Length 65 Ft. Conc. Pile Size 18" Square Steel Pile Size _____ Timber Pile Butt ____ Tip ____

Ground Elevation 0.00 Weight of Drop Hammer _____ Lbs.

Size and Make of Single Acting Power Hammer Delmag D46-02 (Wt of Ram = 10,100 Lbs.)

Size and Make of Double Acting Power Hammer _____

W. A. Potter, Supv. Resident Engineer. Date November 10, 1975

PILE TIP ELEVATION (FT.)	DEPTH OF PILE IN GROUND	SPEED & STROKE OR ENERGY OF HAMMER	NUMBER OF BLOWS	TOTAL PENETRATION (INCHES)	AVERAGE PENETRATION (INCHES)	COMPUTED RESISTANCE (TONS)
-12.00	12	Wt. of Hammer		-	-	-
-13.00	13	5	1	12.00	12.00	4.17
-14.00	14	6	2	12.00	6.00	9.93
-15.00	15	6	2	12.00	6.00	9.93
-16.00	16	6	1	12.00	12.00	5.01
-17.00	17	5.5	2	12.00	6.00	9.11
-18.00	18	5.5	2	12.00	6.00	9.11
-19.00	19	6	2	12.00	6.00	9.93
-20.00	20	6	4	12.00	3.00	19.55
-21.00	21	6	4	12.00	3.00	19.55
-22.00	22	6	4	12.00	3.00	19.55
-23.00	23	6	3	12.00	4.00	14.78
-24.00	24	6.5	5	12.00	2.40	26.26
-25.00	25	6.5	4	12.00	3.00	21.18
-26.00	26	6.5	5	12.00	2.40	26.26
-27.00	27	6.5	5	12.00	2.40	26.26
-28.00	28	6.5	5	12.00	2.40	26.26
-29.00	29	6.5	6	12.00	2.00	31.26
-30.00	30	6.5	6	12.00	2.00	31.26
-31.00	31	6.5	6	12.00	2.00	31.26
-32.00	32	6.5	5	12.00	2.40	26.26
-33.00	33	6.5	6	12.00	2.00	31.26
-34.00	34	6.5	6	12.00	2.00	31.26
-35.00	35	6.5	6	12.00	2.00	31.26
-36.00	36	6.5	7	12.00	1.7143	36.18
-37.00	37	6.5	7	12.00	1.7143	36.18
-38.00	38	6.5	7	12.00	1.7143	36.18
-39.00	39	6.5	7	12.00	1.7143	36.18
-40.00	40	6.5	8	12.00	1.50	41.03
-41.00	41	6.5	8	12.00	1.50	41.03
-42.00	42	6.5	7	12.00	1.7143	36.18
-43.00	43	6.5	8	12.00	1.50	41.03
-44.00	44	6.5	7	12.00	1.7143	36.18
-45.00	45	6.5	7	12.00	1.7143	36.18
-46.00	46	6.5	7	12.00	1.7143	36.18
-47.00	47	6.5	7	12.00	1.7143	36.18
-48.00	48	6.5	6	12.00	2.000	31.26
-49.00	49	6.5	6	12.00	2.00	31.26
-50.00	50	6.5	5	12.00	2.40	26.26

TABLE IV-1. - DRIVING RECORD FOR TEST LOAD PILE AT BENT 29

Bent #29

Texas Highway Department
Form 181 2-57-5m

TEST PILE DATA

Test Pile No. 4

County Chambers Project BRF 749(6) Highway No. 124 Control 367-2-48

Structure or Stream Intracoastal Canal Sta. *187+84 Rt. ~~Bk.~~ 9 Ft. Design Brg. Resist. 60 Tons

Length 65 Ft. Conc. Pile Size 18" Square Steel Pile Size _____ Timber Pile Butt ____ Tip ____

Ground Elevation 0.00 Weight of Drop Hammer _____ Lbs.

Size and Make of Single Acting Power Hammer Delmag D46-02 (Wt of Ram = 10,100 Lbs.)

Size and Make of Double Acting Power Hammer _____

W. A. Potter, Supv. Resident Engineer. Date November 10, 1975

PILE TIP ELEVATION (FT.)	DEPTH OF PILE IN GROUND	SPEED & STROKE OR ENERGY OF HAMMER	NUMBER OF BLOWS	TOTAL PENETRATION (INCHES)	AVERAGE PENETRATION (INCHES)	COMPUTED RESISTANCE (TONS)
-51.00	51	6	6	12.00	2.00	28.86
-52.00	52	6	6	12.00	2.00	28.86
-53.00	53	6	5	12.00	2.40	24.24
-54.00	54	6	7	12.00	1.7143	33.40
-55.00	55	6	7	12.00	1.7143	33.40
-56.00	56	6	6	12.00	2.00	28.86
-57.00	57	6	6	12.00	2.00	28.86
-58.00	58	6	6	12.00	2.00	28.86
-59.00	59	6	6	12.00	2.00	28.86

REMARKS: *Bent No. 29

Formula Used: $P = \frac{2WH}{S+0.1}$

Inspector: Walter L. Poole, Jr.

NOTE:—For distribution, forward one copy to the Austin Office (D-5) for State Projects and Federal Aid Secondary Projects; two copies for Federal Aid Primary and Interstate Projects and one copy for each additional agency involved.

TABLE IV-1. - CONTINUED

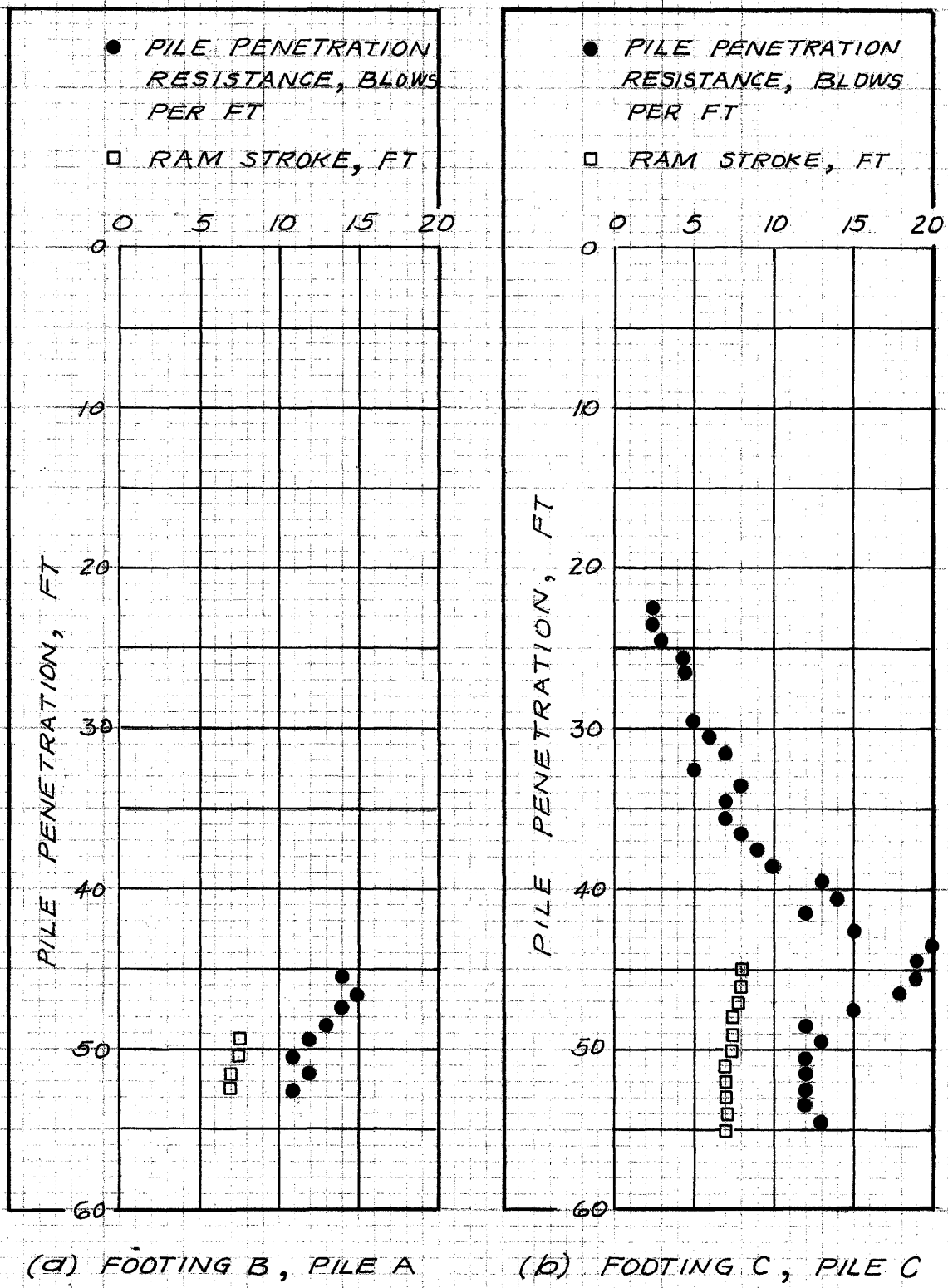

FIG. IV-4. — DRIVING RECORDS FOR INSTRUMENTED PILES AT BENT 34

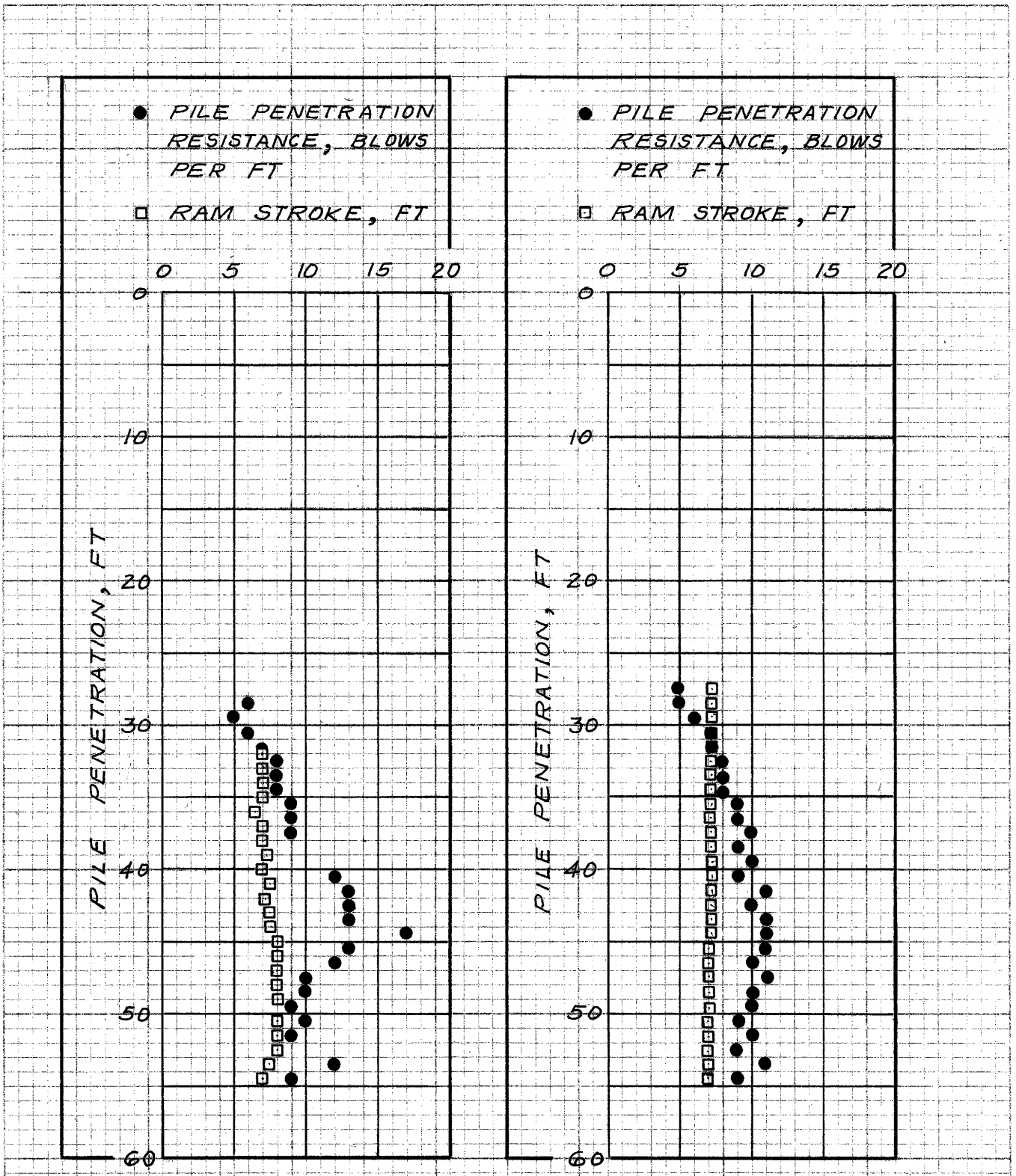

(a) FOOTING C, PILE B (b) FOOTING C, PILE D

FIG. IV-5. — DRIVING RECORDS FOR INSTRUMENTED PILES AT BENT 34

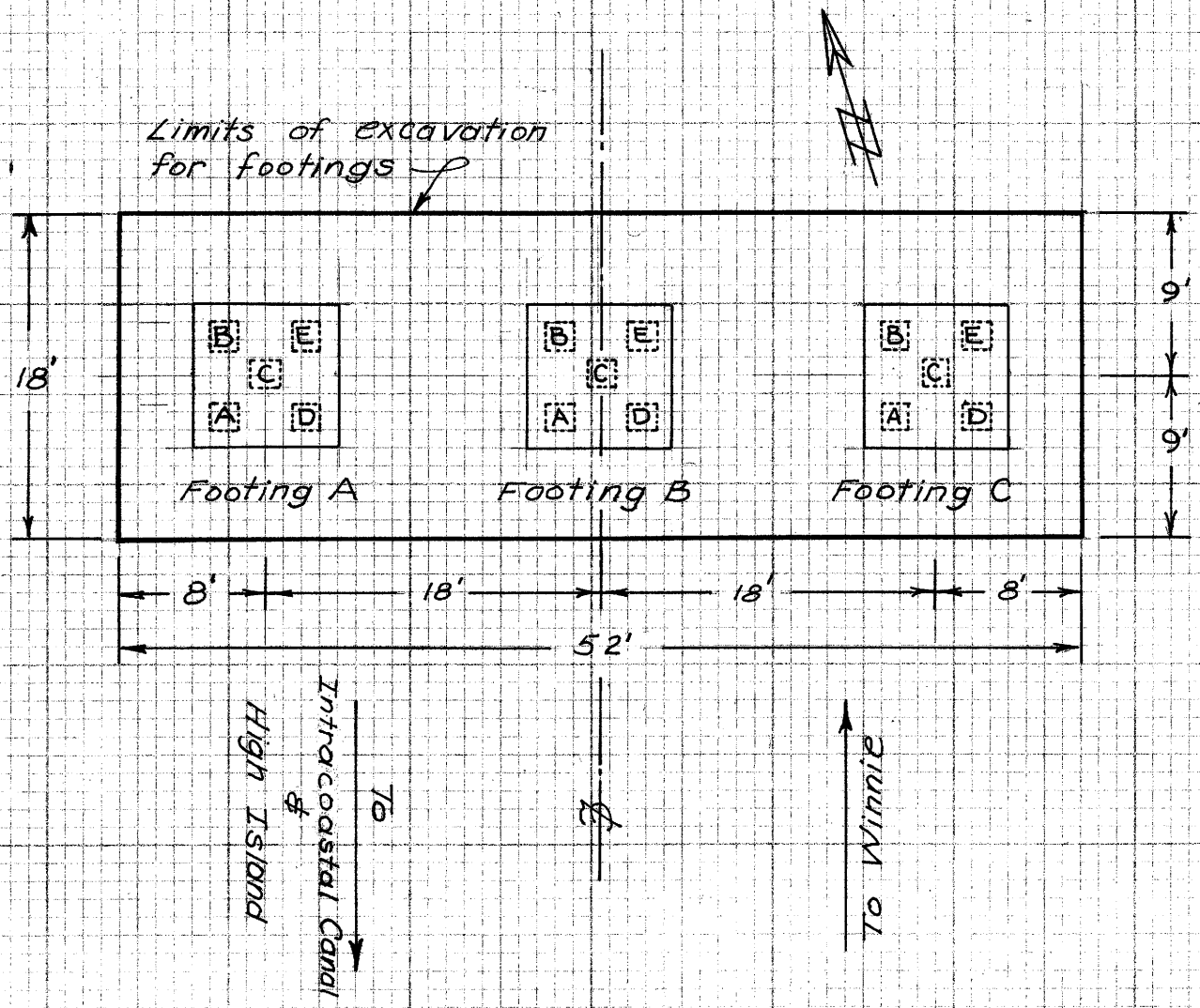

FIG. IV-6. — PLAN VIEW OF EXCAVATION AT BENT 34 SHOWING LETTERING SCHEME FOR IDENTIFICATION OF PILES AND FOOTINGS

Pile Data - Each of the instrumented piles was an 18-in. (460-mm) square concrete pile 55-ft (17-m) long. In order to simulate the pile for purposes of a wave equation analysis, the pile was subdivided into 10 segments, each segment being 5.5-ft (1.7-m) long. The AE/L stiffness of each pile segment was computed to be 27,000 kip/in. (4.7×10^6 kN/m) using a concrete modulus of elasticity of 5.5×10^3 psi (38×10^6 kN/m^2). The first pile segment stiffness was combined with the cushion stiffness using Kirchoff's law, the result being K_3 = 2940 kips/in. (5.1×10^5 kN/m). The weight of each segment is approximately 1.86 kips (844 kg).

Pile Peak Force Measurements - The peak force at the head of the pile during driving was measured by two recording devices, one being the DHT peak force readout unit, the other being the Honeywell Visicorder for recording a continuous record of pile force with respect to time. The strain signal was supplied by two embedment type plastic encapsulated electric resistance strain gages, as discussed in the main text under the section entitled "ALTERNATE TRANSDUCERS FOR CONCRETE PILES - Full Scale Field Tests."

In order to measure the peak force with the DHT readout unit it was first necessary to calibrate the unit. The detailed calibration procedures, although simple, will not be given here. The calibration procedure is given in detail in (4). In order to calculate the required calibration resistor value, Eq (8) in (4) was used. It was necessary to assume reasonable values for the concrete modulus of elasticity and the maximum expected P/A stress in order to solve Eq (8). The values used were $E = 5 \times 10^6$ psi (34×10^6 kN/m^2) and P/A = 2500 psi (17200 kN/m^2) which resulted in a required calibration resistor of 150K ohms. In accordance with the calibration procedure, the next higher calibration

resistor setting on the readout was selected, i.e., switch position No. 7 equaling 232K ohms. It was then necessary to calculate the magnitude of the pile force required to produce an actual strain in the pile that is equivalent to the fictitious strain induced internally in the readout by the calibration resistor. This force was calculated by using the equation given on p. 69 of (4). The parameters entered into the equation were as follows:

R = 300 ohms $\qquad 2R$ = 6 ohms
$E = 5 \times 10^6$ psi (34×10^6 kN/m^2)
A = 324 in.^{2} (0.209 m^2)
cal R = 232K ohms $\qquad N_{eff} = 2 \quad GF = 2.00$

The calculation resulted in a value of P = 545.5 kips (2427 kN) for the calibration setting on the readout. With this value set into the readout, the displayed value during operation is then equal to the actual peak force on the pile in kips. Note that the value of P = 545.5 kips (2427 kN) is also the value of the calibration step trace on the visicorder. It should be further noted that this value is predicated on the assumption that the concrete modulus of elasticity is 5×10^6 psi (34×10^6 kN/m^2). As will be described in greater detail in connection with the wave equation analysis, it appears that the modulus is somewhat greater than assumed. If it were possible to determine the actual modulus the observed peak forces could be corrected simply by multiplying the recorded value by the ratio of the actual modulus to the assumed modulus, since from Eq. (8) it is seen that the calibration force P is directly proportional to the concrete modulus.

Table IV-2 presents the forces recorded during the field tests, based on the assumption that $E_{conc} = 5 \times 10^6$ psi (34×10^6 kN/m^2). The notation used for identifying the piles consists of a number which

TABLE IV-2. - FORCES MEASURED WITH DHT PEAK FORCE READOUT UNIT, IN KIPS (E_{conc} = 5 X 10^6 psi)

Pile 1BA		Pile 2CC		Pile 3CB		Pile 4CD	
Penetration, in ft (1)	Force (2)	Penetration, in ft (3)	Force (4)	Penetration, in ft (5)	Force (6)	Penetration, in ft (7)	Force (8)
↑	247	47-48	322	↑	70	↑	213
	248		348		106		214
Random	281			Random	148	Random	267
	322	48-49	323		214	Readings	224
Readings	295		354	Readings	108		241
	258		327		160		238
	281				244	Penetration	252
	308	49-50	340		171	not	243
Penetration	268		322	Penetration	169	Recorded	274
	322		330		175		245
not	291			not	201	↓	262
	271	50-51	309		210		273
Recorded	302		312	Recorded	218		
	317		346		224	35-40	276
↓	299		309	↓	249		199
	339				254		289
	330	51-52	293		226		306
	333		301		264		287
	354		281		257		320
			306		267		294
46-49	341		320		255		243
	335		295		260		254
	313				264		300
	328	52-53	314		275		306
	304		323		266		319
					272		284
49-51	304	53-55	314		237		
	334		280		302	40-45	308
	334		308		263		310
	290			↓	288		311
	317						302
				35-43	293		303
51-52	312				272		284
	277				292		311
	308				313		309
	334				317		317
					310		320
52-53	314				293		319
	299				277		332
							315
53-55	321			43-44	307		323
	278				292		314
	304				318		306

TABLE IV-2. - CONTINUED

Pile 1BA		Pile 2CC		Pile 3CB		Pile 4CD	
Penetration, in ft (1)	Force (2)	Penetration, in ft (3)	Force (4)	Penetration, in ft (5)	Force (6)	Penetration, in ft (7)	Force (8)
53-55	294			43-44	314	40-45	303
	288						
				44-45	334	45-50	292
					335		317
					347		289
					365		299
					404		304
							312
				45-46	429		319
					422		301
					435		266
					401		280
							283
				46-50	409		293
					430		279
					400		262
					362		
					380	50-52	250
					374		298
					346		287
							270
				50-51	356		285
					311		268
					355		
					363	52-53	268
					364		
					368	53-55	297
							283
				51-52	318		270
					346		

designates the numerical sequence in which the pile was driven, followed by two alphabetic characters designating the footing and the location of the pile in the footing. For example, pile 3CB was the third instrumented pile to be driven, the pile being located on the northwest corner of the easternmost footing (see Fig. IV-6). As indicated in Table IV-2, random readings were made without regard to pile penetration until the pile was within 10 ft to 20 ft (3.0 m to 6.1 m) of final penetration, at which time the recording of penetration was begun and continued to the end of driving.

Fig. IV-7 presents a frequency histogram of the peak forces measured with the DHT readout unit. The vertical scale represents the frequency of occurrence of a given peak force plotted on the horizontal scale. These data indicate that piles 1BA, 2CC, and 4CD were similar as far as the peak force is concerned. Pile 3CB appears to be the exception, having a unimodal frequency distribution as compared to the miltimodal distributions of the other 3 piles, and furthermore the range of the forces appear to be relatively larger in comparison. There were no apparent external differences noted during the actual driving of pile 3CB and the seemingly erratic behavior is so far unexplained.

Table IV-3 presents a summary of the data measured with the DHT readout device, considering only the forces measured during the final 10 ft (3.0 m) of pile penetration. The tabulated values are the median, mean, standard deviation and coefficient of variation of the measured peak forces for each of the piles individually, as well as for the combined forces for all four piles taken collectively. The coefficient of variation is defined herein as the ratio of the standard deviation to the mean.

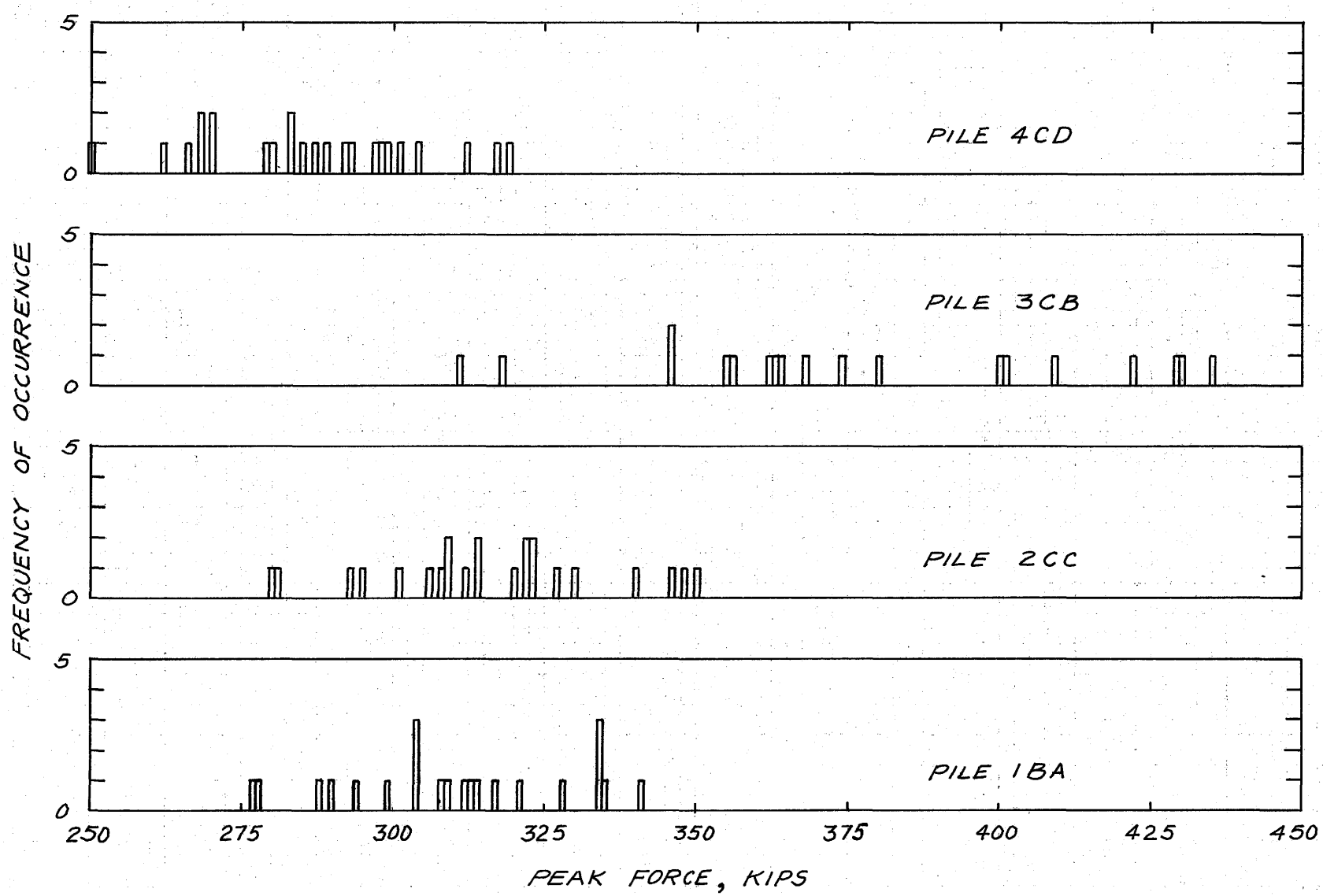

FIG. IV - 7. — FREQUENCY HISTOGRAM OF PEAK PILE FORCES MEASURED WITH THE DHT READOUT UNIT DURING THE LAST 10 FT OF PENETRATION AT BENT 34

TABLE IV-3. - SUMMARY OF FORCES MEASURED WITH DHT READOUT DURING FINAL 10 FT OF PENETRATION

Pile	No. of data points	Range in kips	Median, in kips	Mean, in kips	Standard deviation, in kips	Coefficient of Variation, x 100%
(1)	(2)	(3)	(4)	(5)	(6)	(7)
1BA	22	277-341	311	310.8	18.7	6.0
2CC	23	280-350	314	316.2	19.3	6.1
3CB	19	311-435	368	377.3	36.8	9.8
4CD	24	250-319	286	286.3	17.9	6.3
Comb.	88	250-435		319.9	40.0	12.5

$E_{conc} = 5 \times 10^6$ psi; 1 kip = 4.45 kN; 1 psi = 6.9 kN/m^2

Table IV-4 presents the peak forces obtained from the Visicorder traces, based on the assumption that $E_{conc} = 5 \times 10^6$ psi (34×10^6 kN/m^2). Also given in Table IV-4 are the median, mean, and standard deviation of the measured peak forces for each pile separately, and for the combined data of all four piles collectively. A representative sample of the force-time traces obtained from the Visicorder is presented in Fig. IV-8.

It is of interest to note at this point the comparison between the mean forces determined by the two modes of measurement, viz. the DHT readout and the visicorder. Table IV-5 presents the mean forces recorded with the two systems for each pile individually and for the four piles collectively. Col. 4 of the table shows the ratio of the mean visicorder force to the mean DHT readout force. This comparison shows that the peak forces obtained from the visicorder ranged from about 6% lower to 18% higher than similar readings obtained with the DHT readout; overall the visicorder gave forces that were about 10% higher than the DHT readout forces. Theoretically the two measurement systems should

TABLE IV-4. - SUMMARY OF PEAK PILE FORCES MEASURED WITH VISICORDER

PILE 1BA		PILE 2CC		PILE 3CB		PILE 4CD	
Penetration, in ft	Force, in kips	Penetration, in ft	Force, in kips	Penetration, in ft	Force, in kips	Penetration, in ft	Force, in kips
(1)	(2)	(3)	(4)	(5)	(6)	(7)	(8)
	389	50-51	340	35-40	330	35-40	345
	353	52-53	330	40-43	345	40-45	360
	384			46-50	395	45-50	325
	343			50-55	355	50-52	325
49-51	343						
49-51	358						
MEDIAN = 355.5		MEDIAN = 335		MEDIAN = 350		MEDIAN = 335	
MEAN = 361.7		MEAN = 335		MEAN = 356		MEAN = 338.8	
STD DEV = 20.2		STD DEV= 7.1		STD DEV= 27.8		STD DEV= 17.0	
COEFF OF VAR = 5.6		COEFF OF VAR = 2.1		COEFF OF VAR = 7.8		COEFF OF VAR = 5.0	

Combined data

No. of data points	= 16	Mean	= 351.2 kips
Range	= 325-395 kips	Std dev	= 21.9 kips
Median	= 345 kips	Coeff of var	= 6.2

NOTE: $E_{conc} = 5 \times 10^6$ psi; 1 ft = 0.305m; 1 kip = 4.45 kN
1 psi = 6.9 kN/m^2

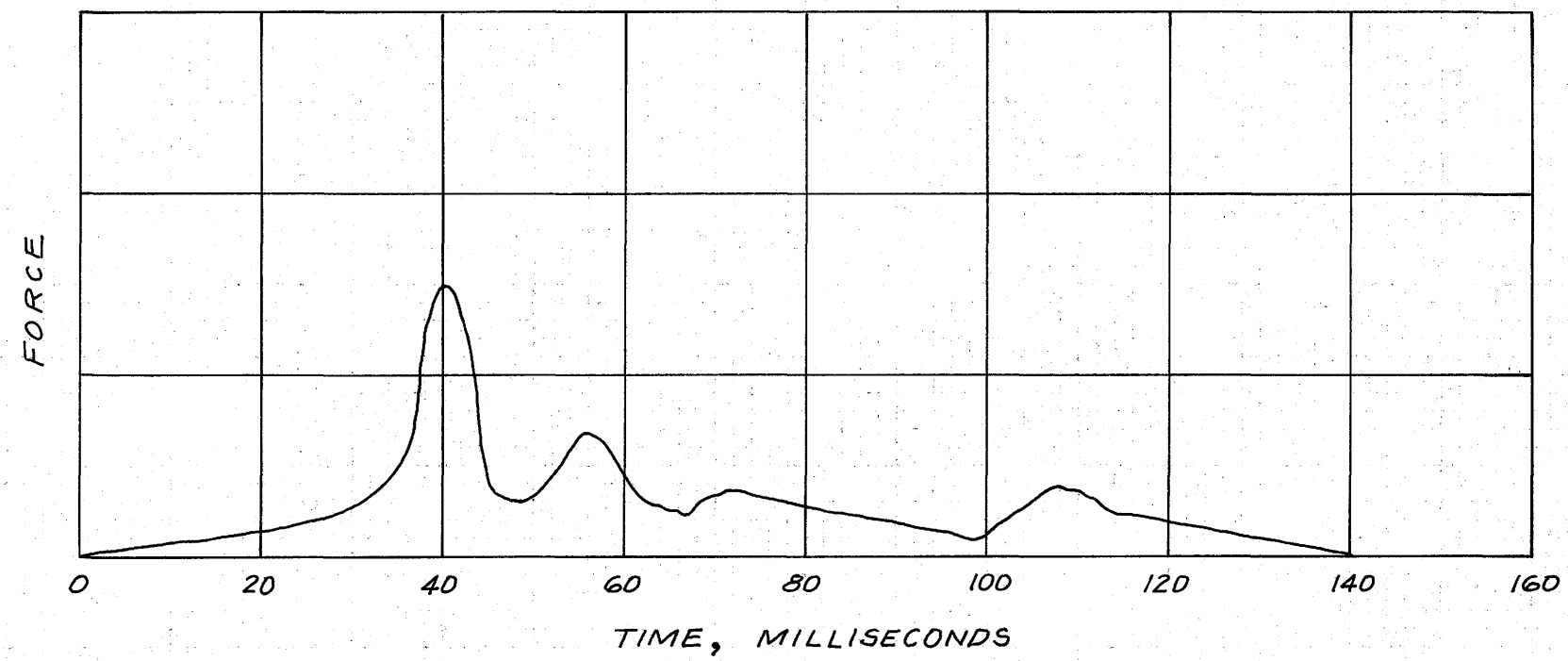

FIG. IV-8. — TYPICAL VISICORDER RECORD OF FORCE AT THE PILE TOP VERSUS TIME, MEASURED ON PILES IN BENT 34

TABLE IV-5. - COMPARISON OF MEAN PEAK FORCES MEASURED BY DHT READOUT AND BY VISICORDER

Pile No.	Mean visicorder force, in kips	Mean DHT readout force, in kips	Ratio (2) ÷ (3)
(1)	(2)	(3)	(4)
1BA	361.7	310.8	1.164
2CC	335.0	316.2	1.059
3CB	356.0	377.3	0.944
4CD	338.8	286.3	1.183
Combined	351.2	319.9	1.098

$E_{conc} = 5 \times 10^6$ psi; 1 kip = 4.45 kN; 1 psi = 6.9 kN/m^2

give the same results because they both utilized an input signal from the same strain gage bridge. Although the variation cannot be definitely associated with any specific cause, it is suggested that the variation is due to the random sampling of the data in connection with the two measurements, i.e., it was not possible to sample exactly the same hammer blow with both systems. Although it appears reasonable to expect the variation due to the above cause to be small, whereas in fact 3 times out of 4 the variation was about 10% on the high side, this variation is not considered to be extreme. In order to select the "best estimate" of the peak pile force for wave equation analysis purposes, it was decided to use the mean peak force measured with the DHT readout because the readout is the system that is to be implemented and used in everyday field work. Therefore 320 kips (1420 kN) was selected as the most representative peak pile force.

Wave Equation Analysis - The determination of pile bearing capacity by wave equation analysis is the primary reason for having the DHT load

cell and readout unit. To achieve this end, the application and utility of a measured peak pile force to a wave equation analysis will be demonstrated with the High Island field test data.

The determination of most of the required input data for the wave equation analysis was covered in some detail in the sections on soil, hammer and pile data. Fig. IV-9 presents a summary of the basic input data. The initial ram velocity was determined from the average ram fall distance for all four piles, the distance being 7 ft (2 m). The port distance to bottom dead center of the ram stroke is 1.77 ft (0.540 m) for the Delmag D46-02, which gives an effective ram drop of 5.23 ft (1.60 m). Neglecting the affect of friction on the ram and using the equation $v = (2\ gh)^{\frac{1}{2}}$ yields an initial ram velocity of 18.4 ft/sec (5.61 m/sec).

Using the input data shown in Fig. IV-9, a wave equation analysis was made with the value of K_3 = 2940 kips/in. (515 x 10^3 kN/m) which represents the combined stiffness of the cushion plus the first pile segment. The static soil resistance, RUT, was taken to be 87.5 tons (779 kN) as this is approximately the value measured by test load at bent 29. Under these conditions the computed force at the head of the pile was 444 tons (3950 kN), whereas the measured force was 160 tons (1420 kN) from the strain gage data. In order to achieve a better agreement between the computed and measured forces, the ram impact velocity was decreased as suggested by Kaiser (2). However, by reducing the velocity to 12.0 ft/sec (3.66 m/sec), which is an unrealistic value for the D46-02 hammer, the computed force at the pile head could only be reduced to 297 tons (2640 kN). Additional wave equation analyses

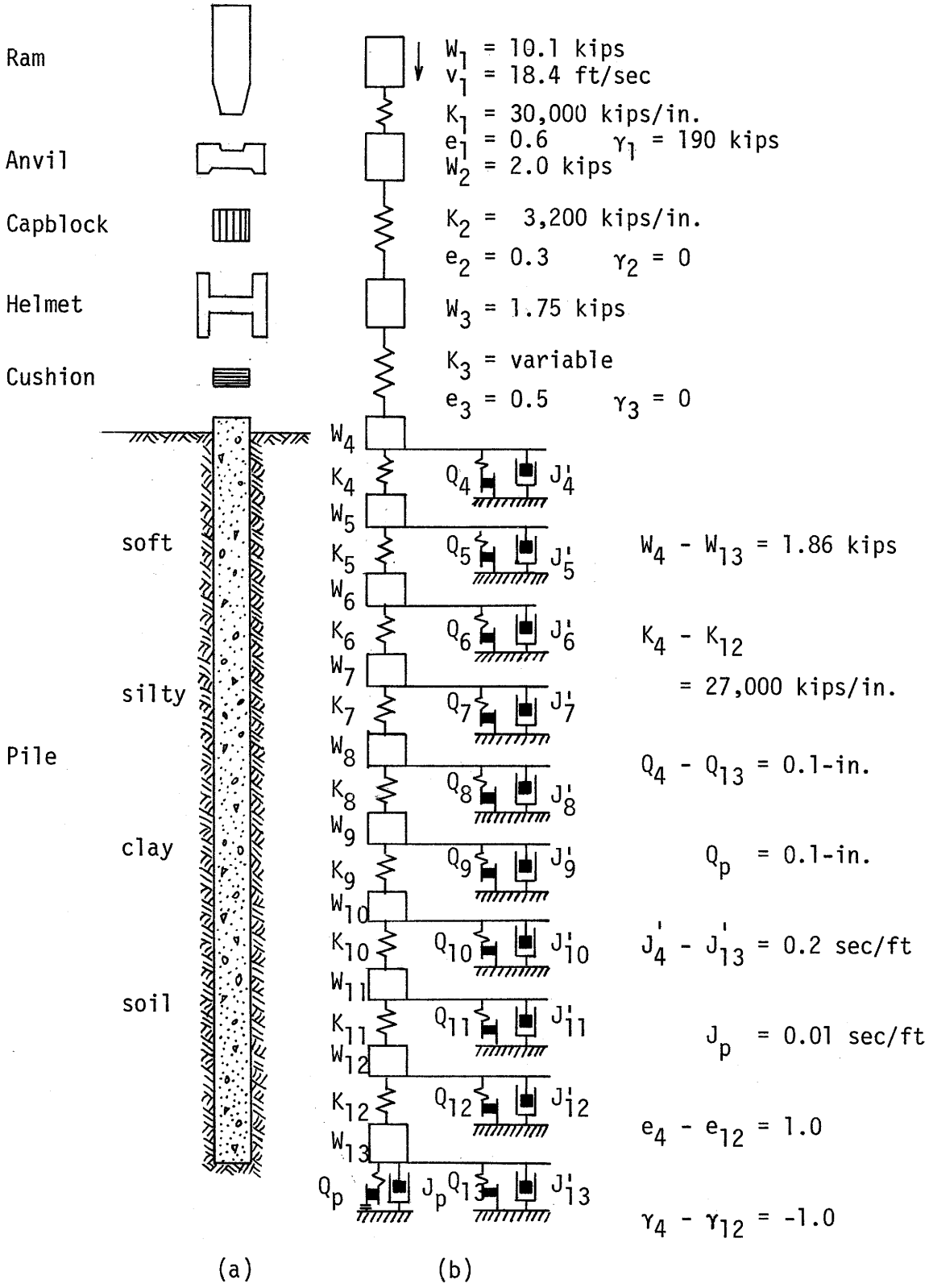

Fig. IV-9. -- Idealization of Hammer-Pile-Soil System for Analysis by the Wave Equation Method. (a) Actual System; (b) Idealized System.

were performed wherein the stiffness value K_3 was reduced, all other data being as shown in Fig. IV-9. By successive trials it was found that a value of K_3= 110 kips/in. (19,300 kN/m) gave a computed force of 158 tons (1410 kN) at the pile head for a soil resistance of 87.5 tons (779 kN). With the value of K_3 = 110 kips/in. bearing graph B of Fig IV-10 was developed. From Fig. IV-10, curve B, it is determined that the predicted pile bearing capacity is 41 tons (360 kN) at 6 blows/ft (20 blows/m) which is the blow count recorded at bent 29 where the test load was conducted. This predicted capacity does not compare favorably with the test load capacity of 90 tons (800 kN). It had been tacitly assumed, based on an examination of the soil profiles at bents 29 and 34, that the two bents were very similar as far as the soil conditions were concerned, therefore they should also be similar with respect to driving conditions, peak forces at the pile head and bearing capacity. On the basis of the wave equation analysis and the recorded blow counts at the two bents it became quite obvious that either the measured field data or the assumption regarding site similarity was in error. The concrete modulus of elasticity had not been determined by lab test, therefore it was quite possible that the modulus could be higher than the 5 x 10^6 psi (34 x 10^6 kN/m^2) value that had been assumed. A new wave equation analysis was conducted with E increased by 60% to 8 x 10^6 psi (55 x 10^6 kN/m^2), which in effect increased the measured peak force by 60% to 256 tons (2280 kN) because the pile force is directly proportional to the modulus ($P = AE\varepsilon$). It was then determined that K_3 = 575 kips/in. (101 x 10^3 kN/m) was required to obtain a computed peak force of 260 tons (2300 kN). The

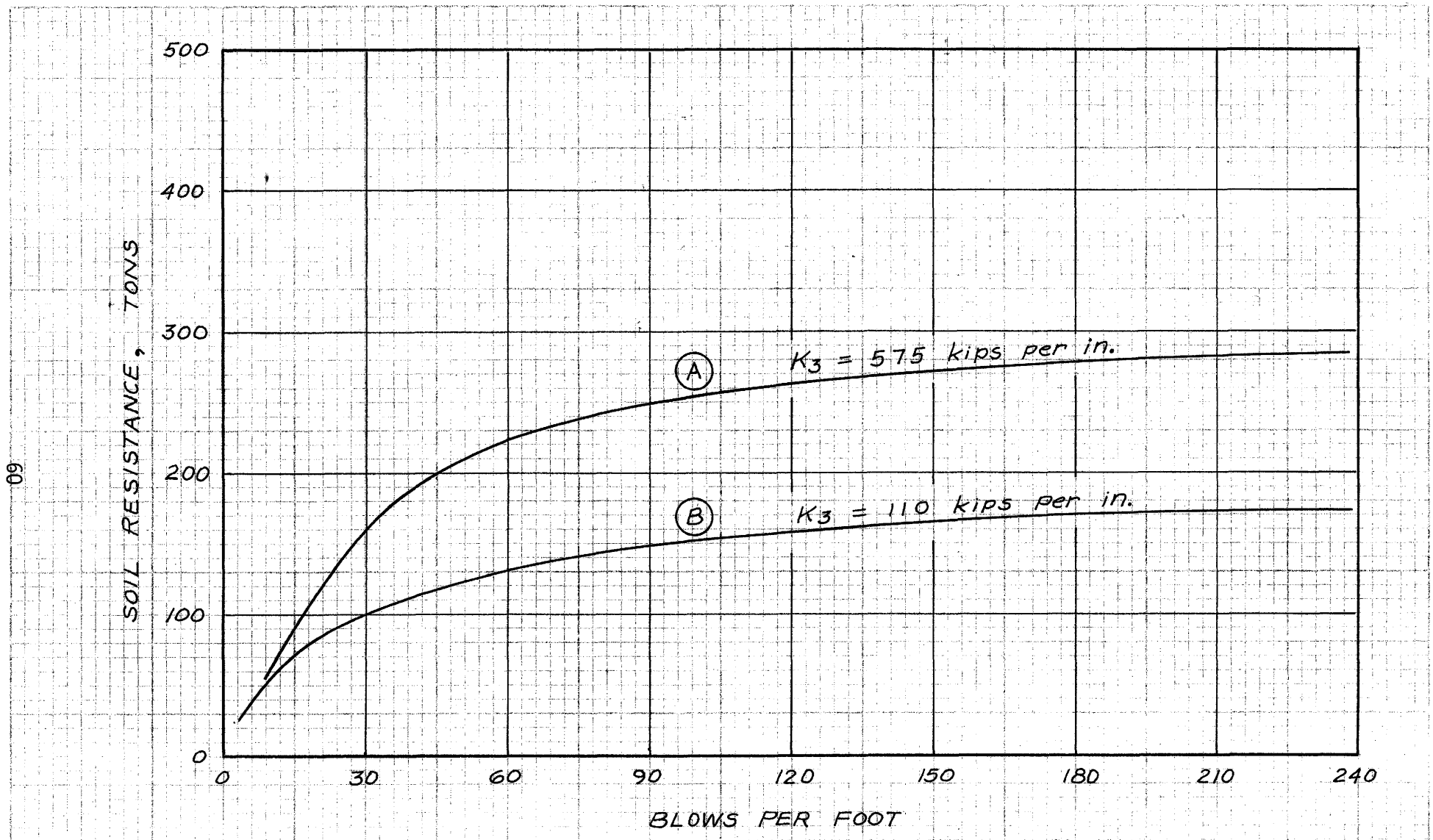

FIG. IV-10. — BEARING GRAPHS FOR 55-FT PILES DRIVEN INTO SOFT SILTY CLAY ON STATE HIGHWAY 124 AT THE INTRACOASTAL CANAL NEAR HIGH ISLAND, TEXAS

TABLE IV-6. - SUMMARY OF PILE TEST LOADING DATA - DHT QUICK TEST LOAD METHOD

County Chambers Structure Intracoastal Canal

Highway No. State 124 Control 367-2-48 Project BRF 749(6)

Date of Test Load	November 17, 1975 (7 day)	
Bent & Test Pile No.	Bent #29 - Test Pile #4	
Location (Station)	187+84	
Description of Pile	18" Square Concrete	
Total Length	65'	
Ground Elevation	0.00	
Btm. of Ftng. Elev.	-0.97	
Pilot Hole Elev.	0.00	
Pile Tip Elev.	-59.00	
Effective Pen.	59.00'	
Soil Type (General)	Soft Wet Clay	
Design Load per Pile	60 Tons	
Type & Size of Hammer	Delmag D46-02	
Dynamic Resistance (ENR)	28.86	
Penetration per Blow	2.0"	
Description Cushion	Capblock	
Type Green Oak	Pine Plywood	
Size 26" Ø	23" (Square)	
Thickness 6"	3"	
	7 day test	0 day test (11/10/75)
Duration of Quick Test Load	47.5 Min	25 Min
Maximum Load On Pile	160 Tons	90 Tons
Gross Settlement	1.84"	1.23"
Net Settlement	1.68"	1.12"
Plunging Failure Load	160 Tons	90 Tons
Ult. Static Bearing Capacity	149.50 Tons	74 Tons
Maximum Proven Design Load	74.75 Tons	37 Tons
"K" Factor (Proven)	2.6	1.3

Remarks:

STATE DEPARTMENT OF HIGHWAYS
AND PUBLIC TRANSPORTATION
District 20
Date 11-17-75

bearing graph obtained with K^3 = 575 kips/in. (101 x 10^3 kN/m) is shown as curve A in Fig. IV-10. From this curve the predicted bearing capacity is again estimated to be about 41 tons (360 kN) because, as is shown in Fig. IV-10, the two bearing graphs are practically congruent at blow counts less than 8 blows/ft (26 blows/m). Note that at 12 blows/ft (39 blows/m), which is the average blow count recorded at bent 34, the predicted bearing capacity from curve A is about 75 tons (670 kN) which is only 15 tons (130 kN) less than the test load value.

By considering the pile stress that corresponds with the measured peak force, the peak force obtained by using E = 8 x 10^6 psi (55 x 10^6 kN/m^2) appears to be more reasonable. In more explicit terms, when E = 5 x 10^6 psi (34 x 10^6 kN/m^2) the peak force of 160 tons (1420 kN) yields a stress of 990 psi (6800 kN/m^2) on the top of the pile. In contrast to this value, using E = 8 x 10^6 psi (55 x 10^6 kN/m^2) and a peak force of 256 tons (2280 kN) yields a pile stress of 1580 psi (10,900 kN/m^2). Although still low in comparison with the usual stress level of about 2000-2500 psi (13,800-17,200 kN/m^2), this value is much more credible than the 990 psi (6800 kN/m^2).

In summary, although it is not possible to definitely establish the most probable cause or source of uncertainty in the analysis of the High Island test data, the data still appear to be indicative of the actual field conditions. In the analysis of these data it was necessary to reduce the cushion-pile combined stiffness by a factor of 5 to achieve reasonable results. Experience with the wave equation method of analysis in other piling applications, both onshore and offshore, indicates that the use of a stiffness reduction factor at the

head of the pile is a rational means of obtaining results that are in closer agreement with field measurements. Although a reduction factor of 3 for concrete piles appears to be most appropriate in the majority of the other cases, a factor of 5 certainly is not beyond reason. In light of these results it is now being recommended that the velocity of the ram not be altered on the first attempt to reconcile wave equation analyses with field measurements or local experience as suggested by Kaiser et al (2). Instead, it is now recommended that a cushion stiffness reduction factor of 3 be applied to the stiffness value that is calculated by using the "book" or "average" values of moduli of elasticity of the common cushion materials. If satisfactory results cannot be achieved by this procedure then it would be permissable to adjust the ram velocity somewhat, provided there is a sound basis for doing so.

APPENDIX V - LABORATORY DATA FROM MODEL TESTS ON ALTERNATE FORCE TRANSDUCING METHOD

Laboratory tests on the alternate peak force transducing means were described in the main text of this report. The correspondence between internally and externally measured strains has been assumed to be linear, therefore it can be described by the equation.

$$\varepsilon_i = a_o + a_1 \varepsilon_e \quad \ldots\ldots\ldots\ldots \quad (V\text{-}1)$$

The notation used in Eq. V-1 is described in the main text.

Table V-1 presents the regression coefficients a_o and a_1 obtained from the regression of ε_i on ε_e. The coefficients are given for the individual test specimens, and for the two types of adhesives that were used. Cols. (6) and (7) give the average coefficients for a given specimen, whereas the final row of data gives the average values obtained for a given type of adhesive.

TABLE V-1. - REGRESSION COEFFICIENTS OBTAINED FROM LABORATORY MODEL TESTS ON INTERNALLY AND EXTERNALLY MOUNTED EMBEDMENT TYPE STRAIN GAGES

	Grout		Epoxy		Average by beam	
Specimen No. (1)	a_o, in microinches per inch (2)	a_1 (3)	a_o, in microinches per inch (4)	a_1 (5)	a_o, in microinches per inch (6)	a_1 (7)
1	0.45087	1.04176	13.8581	1.06660	7.1545	1.05418
2	-4.57299	1.00610	-0.753926	0.983024	-2.66346	0.99456
3	-4.80941	0.985635	-1.38148	0.988629	-3.09544	0.987132
4	-6.43686	0.963985	3.40720	0.949702	-1.51483	0.956844
Average by adhesive	-3.84210	0.99937	3.7825	0.996989	-0.0298	0.99818

TABLE V-2 - RATIO OF EXTERNALLY MEASURED STRAIN TO INTERNALLY MEASURED STRAIN OBTAINED FROM LABORATORY MODEL TESTS

Time	Specimen 1		Specimen 2		Specimen 3		Specimen 4	
	Grout to internal	Epoxy to internal	Grout to internal	Epoxy to internal	Grout to internal	Epoxy to internal	Grout to internal	Epoxy to internal
(1)	(2)	(3)	(4)	(5)	(6)	(7)	(8)	(9)
1	98.20	81.96	108.76	105.80	100.89	99.93	102.73	104.30
2	96.73	87.38	103.49	101.86	102.29	100.33	105.19	104.62
3	96.89	90.45	101.55	101.73	102.05	100.60	104.84	105.33
P	95.98	91.65	100.04	101.70	102.03	101.33	104.00	104.51
4	95.07	91.79	100.26	102.49	104.15	102.58	107.03	103.67
5	94.55	90.13	100.60	102.68	106.15	103.22	109.59	103.21
6	94.03	90.81	97.84	99.00	109.07	104.66	111.38	100.50
Mean	95.92	89.17	101.79	102.18	103.80	101.81	106.39	103.73
σ	1.47	3.50	3.51	2.00	2.90	1.74	3.12	1.58
Avg by beam	92.54		101.99		102.81		105.06	

NOTE: Tabulated values are equal to actual values x 100.

Table V-2 presents the ratio of the externally measured strain to the internally measured strain for the individual specimens, and for the two types of adhesives within each specimen. The tabulated values were obtained by multiplying the actual ratios by 100. Each horizontal row of data represents a strain measurement made at a particular time during the event. Fig V-1 presents a typical strain waveshape over one loading cycle of approximately 30 msec duration. As indicated in Fig. V-1, times 1, 2 and 3 represent the times at which strain readings were selected prior to the occurence of the peak strain; time P represents the time at which the peak strain occurred; and times 4, 5 and 6 correspond to the times at which the strain readings were chosen after

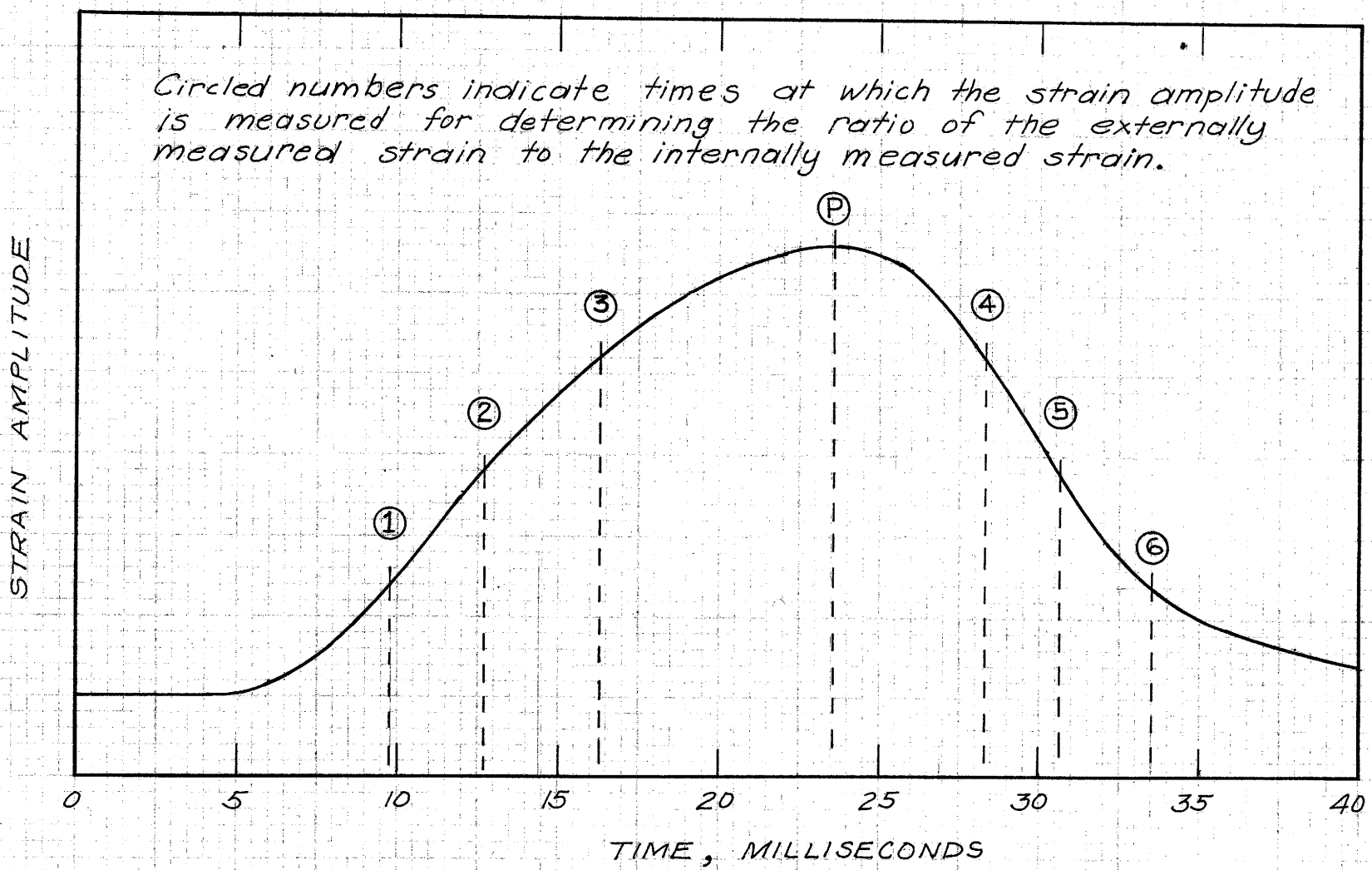

FIG. V-1. — TYPICAL STRAIN WAVESHAPE OBTAINED FROM LABORATORY MODEL TESTS OF THE ALTERNATE FORCE TRANSDUCING METHOD

the occurence of the peak strain. Also tabulated are the mean and standard deviation of the ratios by specimen and by adhesive. The final row of data gives the average ratio by specimen. Note that the ratio for specimen 1 is less than unity, whereas the ratios for specimens 2, 3 and 4 are greater than unity.

NOTES